Metabolic profiling of Lolium perenne shows functional integration of metabolic responses to diverse subtoxic conditions of chemical stress

Anne-Antonella Serra, Ivan Couée, D Renault, Gwenola Gouesbet, Cécile Sulmon

Title:

Metabolic profiling of *Lolium perenne* shows functional integration of metabolic responses to diverse subtoxic conditions of chemical stress

Running title: **Metabolic profiling of chemical stress responses**

Authors:

Anne-Antonella Serra, Ivan Couée, David Renault, Gwenola Gouesbet*, Cécile Sulmon*

*These authors contributed equally to the direction of this study

Institution:

Université de Rennes 1

Centre National de la Recherche Scientifique

UMR CNRS 6553 ECOBIO

Campus de Beaulieu, bâtiment 14A

263 avenue du Général Leclerc

F-35042 Rennes Cedex, France

E-mail addresses:

Anne-Antonella Serra: anne-antonella.serra@univ-rennes1.fr

Ivan Couée: ivan.couee@univ-rennes1.fr

David Renault: david.renault@univ-rennes1.fr

Gwenola Gouesbet: gwenola.gouesbet@univ-rennes1.fr

Cécile Sulmon: cecile.sulmon-maisonneuve@univ-rennes1.fr

Corresponding author:

Cécile Sulmon

Université de Rennes 1

Centre National de la Recherche Scientifique

UMR CNRS 6553 ECOBIO

Campus de Beaulieu, bâtiment 14A

263 avenue du Général Leclerc

F-35042 Rennes Cedex, France

Phone : 33-223235123

Fax : 33-223235026
E-mail : cecile.sulmon-maisonneuve@univ-rennes1.fr

SUMMARY

Long-term adjustment and survival of perennial ryegrass to subtoxic levels of diverse xenobiotic and heavy-metal stresses are associated with major flexibility and complex regulations of central carbon and nitrogen metabolisms.

ABSTRACT

Plant communities are confronted with a great variety of environmental chemical stresses. Characterization of chemical stress in higher plants has often been focused on single or closely-related stressors under acute exposure, or restricted to a selective number of molecular targets. In order to understand plant functioning under chemical stress conditions close to environmental pollution conditions, the C3 grass *Lolium perenne* was subjected to a panel of different chemical stressors (pesticide, pesticide degradation compound, polycyclic aromatic-hydrocarbon, heavy metal) under conditions of seed-level or root-level subtoxic exposure. Physiological and metabolic profiling analysis on roots and shoots revealed that all of these subtoxic chemical stresses resulted in discrete physiological perturbations and complex metabolic shifts. These metabolic shifts involved stressor-specific effects, pointing out to multi-level mechanisms of action, such as the effects of glyphosate and its degradation product aminomethylphosphonic acid on quinate levels. They also involved major generic effects that linked all of the subtoxic chemical stresses with major modifications of nitrogen metabolism, especially affecting asparagine, and of photorespiration, especially affecting alanine and glycerate. Stress-related physiological effects and metabolic adjustments were shown to be integrated through a complex network of metabolic correlations converging on asparagine, leucine, serine, and glucose-6-phosphate, which could be potentially modulated by differential dynamics and interconversion of soluble sugars (sucrose, trehalose, glucose). Underlying metabolic, regulatory and signalling mechanisms linking these subtoxic chemical stresses with a generic impact on nitrogen metabolism and photorespiration are discussed in relation with carbohydrate and low energy sensing.

KEY WORDS

AMPA, carbon-nitrogen balance, copper, glyphosate, phytoremediation, polycyclic aromatic hydrocarbon, residual pollution, perennial ryegrass, tebuconazole, xenobiotics

ABBREVIATIONS

AMPA, aminomethylphosphonic acid; BCAA, branched chain amino acids; Cu, copper; F, fluoranthene; Fru, fructose; Fru-6-P, fructose-6-phosphate; G, glyphosate; Glc, glucose; Glc-6-P, glucose-6-phosphate; GT, combination of glyphosate and tebuconazole; HCA, hierarchical cluster analysis; PAH, polycyclic aromatic hydrocarbon; PCA, principal component analysis; PSII, photosystem II; Suc, sucrose; T, tebuconazole; TCA, tricarboxylic acids; Tre, trehalose; Tre-6-P, trehalose-6-phosphate.

INTRODUCTION

Modern agriculture uses large amounts of numerous pesticides in order to control pests and weeds, and to get around resistance mechanisms of target organisms (Helander et al., 2012). Various processes (drift, runoff, leaching) lead to contamination of terrestrial and aquatic environments by mixtures of chemicals, mainly pesticides, pesticide degradation products, and adjuvants (Dévier et al., 2011; Helander et al., 2012), but also metals (Bidar et al., 2009) and polycyclic aromatic hydrocarbons (PAH) (Kreslavski et al., 2014). Non-target plants can suffer direct damages by chemicals because of their sessile lifestyle. However, the overall effects of these complex, diffuse, and chronic chemical pollutions are difficult to predict (Dévier et al., 2011). Most studies focus on the effects of a restricted number of pollutants, mainly heavy metals and plant-targeting chemicals such as herbicides, whereas better understanding of chemical stress effects requires that a much greater number of chemical stressors, and their corresponding degradation products, be studied. Moreover, exposure protocols do not necessarily reflect conditions of environmental pollution. For most compounds, the mode of action and biological effects of low-level and multiple-stress exposure may differ from effects of toxic or lethal contamination and remain poorly understood. Serra et al. (2013) have shown that, under environmentally-relevant contamination levels, xenobiotics and associated degradation products induced cryptic metabolic perturbations in *Arabidopsis thaliana*, in relation with non-target and signalling effects. These perturbations highlighted complex interactive effects, whether positive or negative, between structurally-different xenobiotics.

Chemical stress induces different responses according to the ability of plant species or ecotypes to integrate stress signals and develop coordinated molecular responses (Ramel et al., 2012; Couée et al., 2013). Perennial ryegrass, *Lolium perenne*, which is the most widely grown grass in temperate regions and a primary food source for grazing ruminants (Barbehenn et al., 2004), has been reported to be tolerant to diverse chemical stressors (Dear et al., 2006; Bidar et al., 2009; D'Orazio et al., 2013). It also accelerates degradation of contaminants in soils (Krutz et al., 2005; D'Orazio et al., 2013), and plays important roles in improving remediation of heavy-metal-contaminated soils (Bidar et al., 2009). *Lolium perenne* has been commonly used in revegetation and phytoremediation projects (Bidar et al., 2009; Hu et al., 2012), and in vegetative filter strips (Krutz et al., 2005). However, mechanisms involved in Lolium tolerance to chemical stressors have not been elucidated, thus highlighting the need for without *a priori* approaches such as metabolomics.

In order to characterize chemical stress responses, *Lolium perenne* was subjected to subtoxic levels of contrasted chemical stressors : (i) the widely used broad-spectrum herbicide glyphosate (Helander et al., 2012), which inhibits aromatic amino acid production through inhibition of 5-enolpyruvylshikimate-3-phosphate synthase (EPSPS) in the shikimate pathway, (ii) its degradation product aminomethylphosphonic acid (AMPA), which may interact with glycine metabolism (Serra et al., 2013), (iii) the triazole fungicide tebuconazole, whether alone or in association with glyphosate, (iv) the PAH molecule fluoranthene, and (iv) the heavy metal copper. Exposure of germinating seeds and root systems, and different modalities of treatment, were used to reflect realistic conditions of environmental exposure (Serra et al., 2013). Plant responses were dissected by physiological and metabolomic analysis (Obata and Fernie, 2012) in order to highlight significant stress-induced shifts in Lolium metabolic profiles, and to identify chemical stressor-specific and generic responses to chemical stress.

MATERIALS AND METHODS

Plant material and growth conditions

Seeds of *Lolium perenne* (Brio cultivar) were washed in ethanol and surface-sterilized in bayrochlore (20 g L^{-1} in water) containing 0.05% tween (v/v) for 20 min and rinsed five times in sterilized water. Moistened seeds were placed in Petri dishes in the dark at 4°C for 7 d in order to break dormancy and homogenize germination. Imbibed seeds were sown on pieces of gauze and placed at the top of sterile tubes containing liquid growth medium. Gauze pieces were moistened by soaking gauze edges into culture medium. Germination and hydroponic growth were carried out under axenic conditions in a control growth chamber at 22°C/20°C under a 16 h light (6000 lux)/8 h dark regime. Growth solution consisted of Hoagland basal salt mix (No.2, Caisson Laboratories, North Logan, UT, USA) adjusted to pH 6. Direct exposure to chemicals was carried out by sowing seeds on chemical-stressor-containing growth medium. Developmental and physiological parameters were measured after 11 d of growth. Transfer experiments consisted in root-level shock exposure of young plants at the same stage of photosynthetic development. After 7 d of growth under control conditions, gauze pieces supporting seedlings were transferred to fresh growth solution containing chemical stressors. Developmental and physiological parameters were measured 4 d later, thus corresponding to 11 d of total growth. Metabolite profiling of seedlings was carried out after direct and transfer exposures. Different chemical treatments were applied: the broad-spectrum herbicide glyphosate (G, 1 µM), its degradation product aminomethylphosphonic acid, AMPA (A, 50 µM), the fungicide tebuconazole (T, 4 µM), the PAH fluoranthene (F, 500 µM), copper (Cu, 6 µM) and a combination of glyphosate and tebuconazole (GT, 1 µM and 4 µM respectively). In order to characterize long-term effects, developmental and physiological parameters were also measured after 30 d of growth under direct exposure to chemical stress. For these experiments, control and contaminated growth solutions were renewed every 11 d. All of these experiments were carried out with at least 5 independent replicates, each consisting of at least 10 plantlets.

Analysis of growth and photosynthetic parameters

Seedlings were aligned on glass plates and photographed. Lengths of main root and elongating leaf were measured using ImageJ software. Pigment contents (chlorophylls and total carotenoids) and maximum photosystem II (PSII) efficiency (F_v/F_m) were quantified as described in Serra et al. (2013).

Metabolic profiling

Roots and leaves of seedlings were collected just before start of daylight period, freeze-dried, ground in liquid nitrogen and stored at -20°C until use. For each sample, five mg of powder was suspended in 600 μL of methanol:chloroform solution (2:1, v/v) and mixed for 1.5 min. Samples were transferred to -20°C for 10 min before adding 400 μL of cold (4°C) water. Samples were mixed vigorously for 1 min, and centrifuged twice for 5 min at 4,000 *g* (4°C). One hundred and twenty μL of upper aqueous phase, containing polar metabolites, were transferred to chromatographic glass vials and vacuum-dried (MiVac, Genevac Ltd., Ipswitch, England). Derivatization of extracts was conducted as previously described (Serra et al., 2013; Supplementary Method S1), using a CTC CombiPal autosampler (GERSTEL GmbH and Co.KG, Mülheim an der Ruhr, Germany), ensuring identical derivatization time and process for all samples. Extracts were analyzed using gas chromatography mass spectrometry (GC/MS). GC/MS system consisted of a Trace GC Ultra chromatograph and a Trace DSQII quadrupole mass spectrometer (Thermo Fisher Scientific Inc, Waltham, MA, USA). Parameters of injection and chromatography were similar to those described in Serra et al. (2013) (Supplementary Method S1). Detection was achieved using electron impact ionization. Temperature of the ion source was set at 250°C and MS transfer line at 300°C. Peaks were accurately annotated using mass spectra (two specific ions) and retention times. Calibration curves were established with 61 pure reference compounds (Supplementary Table S1) at 1, 2, 5, 10, 20, 50, 100, 200, 500, 750, 1000, 1500 and 2000 µM. Each metabolite was quantified according to its corresponding calibration curve, using XCalibur v2.0.7 software (Thermo Fisher Scientific Inc, Waltham, MA, USA) and expressed in nmol per mg dry weight (DW).

Statistical analysis

Physiological and metabolic parameters were measured on at least 5 independent replicates of at least 10 individual plantlets. Statistical analyses were carried out with version 3.0.1 of R software. Pairwise comparisons of means used the non-parametric Mann-Whitney-Wilcoxon test. In order to characterize relationships between treatments and responses, principal component analyses (PCAs), based on correlation matrix of averages (Ramel et al., 2009; Serra et al., 2013), and hierarchical classifications were carried out using the FactoMineR package of R. In order to compare variations between treatments, relative levels of responses against control condition were calculated using $\log_2$(ratio). Metabolic responses between treatments were compared by performing heatmap and hierarchical clustering with EPCLUST

197 software using correlation measure-based distances and average linkage. Pair-wise
198 physiological trait-physiological trait, physiological trait-metabolite, and metabolite-
199 metabolite correlations were determined by Pearson correlation analysis.
200

RESULTS

Effects of subtoxic levels of environmental pollutants on growth and development

The experimental set-up involved root application of chemical stressors and parallel analysis of root growth and leaf growth, which, in *Lolium perenne*, respectively rely on the root apex (Gonthier and Francis, 1989) and on the base of the growing leaf (Kavanová et al., 2008). Chemical stressors were applied to germinating seeds and root systems at no-observed-adverse-effect-levels (NOAEL; Dorato and Engelhardt, 2005) for PSII efficiency, chlorophyll levels, carotenoid levels, and root growth under conditions of transfer exposure, where seedlings grown during 7 d in control medium were subjected to root-level application of chemical stressors during 4 d (Fig. 1A-D). These levels of chemical stressors were at least 20-fold lower than EC (effect concentration)50 values for these parameters under conditions of transfer exposure. Such levels also corresponded to no-observed-adverse-effect-levels for PSII efficiency under direct exposure (Fig. 1H), where germination and seedling growth occurred in the presence of chemical stressors. However, direct exposure conditions had a much greater impact on root length (Fig. 1E), leaf length (Fig. 1F), and photosynthetic pigments (Fig. 1G). Leaf length responses under direct exposure showed the same trend as those observed under transfer exposure, thus indicating that transfer and direct exposures reflected different intensities of chemical stress (Fig. 1B, F). However, in a study of long-term (30 day) growth, *Lolium perenne* seedlings maintained development under these levels of chemical stress, or even escaped major root growth inhibition in the case of AMPA, thus confirming that exposures to chemical stress were subtoxic (Fig. 2).

The impact of treatments depended on type of pollutant, on physiological trait and on modality of chemical exposure (Fig. 1). Root length was particularly responsive to chemical stress under conditions of direct exposure, with all of the chemical treatments inducing significant decrease of growth, except fluoranthene which induced increase of root length (Fig. 1E). Differences of root length between controls of direct and transfer exposure experiments suggested that root growth was sensitive to mechanical processes that may occur during transfer protocol. However, these effects did not result in greater sensitivity to chemical stress (Fig. 1A, E). Direct exposure to copper, glyphosate and its degradation product AMPA showed the same extent of negative impact for root length (Fig. 1E) and photosynthetic pigment levels (Fig. 1G), without affecting leaf length (Fig. 1F). Leaf length was slightly decreased by fluoranthene, thus contrasting with its positive effect on root length.

Glyphosate-tebuconazole mixture (GT) induced a more negative effect on root length than observed for each pollutant alone, although the combined effect was not strictly additive (Fig. 1E). In contrast, length of elongating leaves was similarly negatively affected by tebuconazole and glyphosate-tebuconazole mixture whereas glyphosate, alone or in combination with tebuconazole, did not have any effect (Fig. 1F). Chlorophyll levels were negatively affected by glyphosate, whereas tebuconazole showed a positive effect and lifted the negative effect of glyphosate (Fig. 1G). Such differential responses to these treatments were observed for PSII efficiency with no effect of glyphosate and glyphosate-tebuconazole mixture (Fig. 1H). PSII efficiency thus showed no adverse effect of chemical stress, with only AMPA and tebuconazole inducing a slight increase (Fig. 1H). Maintenance of PSII efficiency at or above control level indicated that photosynthesis remained active in the presence of the different chemicals under the conditions of exposure applied. The present range of chemical stresses therefore seemed to act primarily on growth and development rather than on photosynthesis. Comparison of effects of direct chemical stress on root length and leaf length indicated that glyphosate, AMPA and copper had stronger impacts on root growth, whereas tebuconazole and, to a lesser extent, fluoranthene, had stronger impacts on leaf growth (Fig. 1E, F).

Subtoxic levels of chemical stressors cause major metabolic shifts

Metabolomic analysis of a set of 61 metabolites was performed to reveal discriminant components of metabolic responses to chemical stress. Root and leaf metabolic profiles, resulting from treatments and exposure modalities, were analysed using PCA and associated hierarchical classification. Major metabolic variations separated samples into four response patterns corresponding to each kind of tissues and exposure conditions (Supplementary Figure S1). Metabolic patterns were determined firstly by the nature of the tissue (root or leaf), then by the type of chemical stress exposure, and finally by the nature of the chemical stressor (Supplementary Figure S1), showing that subtoxic chemical stress did not deeply modify general metabolic signatures of organs and exposure modalities.

Metabolic responses were separately analysed (Fig. 3) for each type of exposure and for each organ. All of the chemical stressors caused major metabolic variations in both roots and leaves, whatever the type of exposure. Under conditions of transfer exposure, chemical stressors induced metabolic changes (Fig. 3A, B) in the absence of significant physiological impact (Fig. 1). Copper, glyphosate or its degradation product AMPA caused, under transfer exposure, important metabolic changes in leaves (Fig. 3B) without any physiological effect on leaf growth or photosynthesis (Fig. 1B, D). Under conditions of direct exposure, chemical

stressors induced metabolic changes in the absence of significant impact on photosynthesis (Fig. 1G, H). Some response patterns showed close similarities: in root tissues, transfer and direct exposures resulted in great proximity for control and AMPA, and for glyphosate and glyphosate-tebuconazole mixture (Fig. 3A, C). In contrast, the distance between fluoranthene and tebuconazole greatly differed between transfer and direct exposures in the case of root tissues. Divergences in metabolic profiles of potentially close chemical treatments were also found. The glyphosate degradation product AMPA was never associated to its parent compound glyphosate (Fig. 3). Similarly, tebuconazole was disconnected from glyphosate-tebuconazole mixture, despite their close physiological impacts (Figs 1, 3). Finally, in some cases, such as the effects of AMPA on root or of glyphosate-tebuconazole mixture on leaf, global metabolic patterns were close to the control (Fig. 3C, D) despite major physiological effects (Fig. 1E, F).

Coordination of metabolome changes under conditions of subtoxic chemical stress

Among the 61 metabolites that were analysed and quantified, 42 showed significant variations in relation with at least one of the chemical stress treatments. Variations of these 42 metabolites relatively to control [$\log_2$(ratio)] were classified by hierarchical cluster analysis (HCA) in order to define for each metabolite a pattern of chemical stress response across the 6 different stressors, the 2 modalities of exposure and the 2 organs (Fig. 4). This HCA of the 24 analyses separated metabolites into distinct clusters and subclusters of chemical stress responses that were grouped into 8 general clusters (Fig. 4). Several clusters were characterised by strong relationships between co-metabolites, such as tight clustering of TCA (citrate, succinate, fumarate; cluster F), of fructose (Fru) and glucose (Glc) (cluster G), or of Fru-6-P and Glc-6-P (cluster C). On the other hand, clustering of co-metabolites and of unrelated metabolites, such as Trp and inositol (cluster F), pointed out to potential regulatory networks (Fig. 4).

Highly-contrasted clusters, such as clusters A and B on one hand, and clusters G and H on the other hand, were characterized, respectively, by general increase and general decrease of metabolite levels in response to chemical stressors. The N-rich amino acid Asn (cluster A) showed significant increase across most of the conditions, thus indicating that nitrogen re-distribution and mobilization were important features of chemical stress response in *L. perenne*. Clustering of Met with Asn could be ascribed to its positive variations, which were however much more limited than these of Asn, and to the absence of major negative variations. Cluster B consisted of a set of amino acids including all of the branched-chain

amino acids (Leu, Ile, Val), two aromatic amino acids (Tyr, Phe), and Lys, in association with glycerol and phosphate. It was characterized by common increase in leaf across all chemical stressors in at least one exposure condition. Moreover, cluster B metabolites increased in roots across several chemical stressors (G under direct exposure, and GT, T, and F under both transfer and direct exposures), which may also reflect the importance of root metabolism perturbations under conditions of subtoxic chemical stress (Fig. 5, Supplementary Figure S2). In contrast, ribose and glycerate in, respectively, clusters G and H showed significant decrease across most of the conditions. Moreover, the ribose-associated cluster, as well as the glycerate-associated cluster, comprised stress-related metabolites [gamma aminobutyric acid (GABA), Pro, pipecolate] thus suggesting that chemical stress responses involved remodelling of general abiotic stress responses. Variations of Ala in cluster H may be in line with remodelling of nitrogen metabolism that was highlighted by clusters A and B.

Metabolites from cluster C to cluster F exhibited varied responses of increase or decrease depending on treatments. Some compounds showed changes of very low amplitude. This was especially the case for arabitol and sorbitol (cluster D). In contrast, all of the chemical stressors increased lactate levels (cluster D) in both roots and leaves, in at least one modality of exposure, thus pointing out to glycolysis and energy dysfunction. Cluster E comprised a set of amino acids, including Asn co-metabolite Asp, and other N-rich compounds, such as the polyamine precursor ornithine and the polyamine putrescine. Interestingly, this cluster of amino-compounds included the disaccharides Suc and Tre, thus indicating potential importance of carbon and nitrogen relationships.

Specific effects of chemical stressors on metabolite levels

Some compounds showed contrasted variations according to the nature of chemical stressor, thus giving important insights into specific effects of a given chemical (Table 1). In addition to inducing the highest increase of Asn levels (5.7 fold in leaves, Fig. 5, Supplementary Figure S2), AMPA led to a strong decrease of quinate, a shikimate pathway component, in leaves (3.6-fold, Fig. 5, Supplementary Figure S2). In contrast, glyphosate, which targets a key step of shikimate pathway and aromatic amino acid synthesis, caused significant increase of quinate levels in roots, but not in leaves, either alone or in association with tebuconazole (Fig. 5, Supplementary Figure S2). Such specific variations of quinate suggested particular interference of glyphosate and AMPA with the shikimate pathway, despite the absence of major effects on levels of aromatic amino acids (Phe, Tyr, Trp) (Fig. 5, Supplementary Figure S2). Another striking effect of AMPA was a nearly 2-fold decrease of cell wall metabolite

arabinose in roots (Fig. 5, Supplementary Figure S2). Significant decrease of citrate and/or succinate was observed in roots of tebuconazole- and copper-treated plants, thus suggesting TCA cycle depression and mitochondrial respiration dysfunction (Fig. 5). Fluoranthene treatment was characterised, under conditions of transfer exposure, by accumulation of Fru, Glc, and Ser in roots and leaves, confirming major changes in carbon and nitrogen metabolisms (Table 1, Fig. 4, Supplementary Figure S2). Accumulation of Pro and soluble sugars in fluoranthene-treated leaves pointed out to possible osmotic stress, although the levels of other metabolic markers of osmotic stress response, such as polyols, were not affected (Figs 4, 5). Fluoranthene-enhanced root growth, associated with accumulation of cell wall metabolite arabinose in roots under transfer exposure, may thus represent increased water exploration resulting from osmotic stress response (Figs 1, 4, Supplementary Figure S2). Action of fluoranthene was also characterised by global increase of ethanolamine, potentially indicating changes in phospholipid metabolism under fluoranthene treatments (Supplementary Figure S2).

Identification of metabolic drivers of physiological responses to chemical stress

In order to determine whether physiological responses to chemical stress were related to metabolic changes, organ-specific trait-metabolite Pearson correlations were carried out (Fig. 6, Supplementary Table S2). This correlation approach highlighted global trends in relationships between metabolites and trait responses, rather than chemical stressor specificities. Leaf length was significantly negatively correlated to only one metabolite in leaves, Glc-6-P. In contrast, leaf chlorophyll level was positively correlated to Glc-6-P, and also positively correlated to several metabolites of cluster B (Fig. 4), mainly represented by amino acids (Val, Leu, Phe, Lys, Tyr) and glycerol, to putrescine (cluster E), to arabinose (cluster F), and to pipecolate (cluster H) (Fig. 6, Supplementary Table S2). Putrescine and pipecolate are metabolites that generally increase under stress (Hummel et al., 2004; Servillo et al., 2012). However, under chemical treatments inducing significant, but limited, pigment loss (A, G, Cu; Fig. 1G), their levels were decreased (Supplementary Figure S2). Thus, in accordance with chlorophyll-amino acid correlations (Fig. 6), responses to chemical stress in *Lolium perenne* were related to carbon and nitrogen metabolic rearrangement rather than to induction of stress response metabolic pathways. In contrast, under tebuconazole treatment, which increases chlorophyll levels (Fig. 1C, G), increase of these amino acids may indicate metabolic adaptation rather than proteolysis-related sensitivity (Fig. 5, Supplementary Figure S2).

Leaf length was negatively correlated to several metabolites in root, the most highly correlated being the amino acids Asn (cluster A), Lys, Ile, and Tyr (cluster B) (Fig. 6, Supplementary Table S2). Although links between metabolite levels in root and leaf growth were not direct, such strong negative correlations with amino acids, in particular with N-rich amino acids such as Asn and Lys, highlighted the importance of root-shoot relationships under conditions of chemical stress. A negative correlation was also found with Ser (cluster E), which is a central amino acid involved in photorespiration and in synthesis of glutathione components.

No significant correlation was found between root length and metabolite levels in roots. However, root length exhibited positive correlations with two metabolites quantified in leaves, Pro (cluster G) and quinate (cluster D) (Fig. 6, Supplementary Table S2). These positive correlations indicated that negative effects of chemical stress on root length were associated with decrease of Pro or quinate levels in leaves, although their accumulation has been reported under abiotic or chemical (herbicide, allelopathic compounds) stresses in *Arabidopsis thaliana*, *Nicotiana tabacum*, and *Pisum sativum* (Verbruggen and Hermans, 2008; Orcaray et al., 2010). Variations of Pro and quinate levels in leaves thus reflected a reorientation of leaf metabolic pathways in relation to root growth impacts. Since Pro is one end-product of amino acid synthesis, and quinate is a reserve compound of the shikimate pathway for aromatic acid synthesis (Orcaray et al., 2010), these variations may reflect perturbations of root-shoot nitrogen dynamics.

Metabolite-metabolite correlations highlight the importance of carbon-nitrogen regulations

In order to reveal metabolic networks involved in chemical stress responses, a global pair-wise metabolite-metabolite correlation matrix was calculated (Supplementary Table S3), by Pearson correlation analysis of the complete set of organ- and modality-related metabolite data. Most of the physiological trait-correlated metabolites (Fig. 6) were correlated ($p < 0.05$), mainly positively, with a range of metabolites across the eight clusters (Figs 7, 8). Among these fifteen metabolites, eleven metabolites (Leu, Lys, Val, Tyr, Phe, Ile, quinate, Ser, arabinose, Pro, and pipecolate) exhibited similar or close correlation networks (Supplementary Table S3), mainly integrating amino acids (Met, Ile, Tyr, Leu, Lys, Val, Phe, Ser, Thr, Gly, Asp, Glu, Trp, Ala), carbohydrate metabolism compounds (Glc, Fru, Tre, TCA), stress metabolites (arabitol, inositol, Pro, GABA, pipecolate), and compounds such as arabinose, ethanolamine and quinate. Putrescine exhibited a close, but more restricted, correlation profile, with only ten correlations involving amino acids, TCA, and stress

metabolites. The least correlated metabolite was Asn, which exhibited five correlations, mainly with metabolically-close amino acids such as its direct precursor Asp and also Ser, Thr, and Ile. Except for copper and glyphosate under transfer exposure, chemical stressors induced Asn accumulation, which was almost systematically correlated to increase of these metabolites (Figs 5, 7, Supplementary Figure S2), thus confirming predominant roles for Asn and nitrogen metabolism in chemical stress responses of *L. perenne*. This correlation level observed in the global matrix was extended by considering organ-specific correlation matrices. Asn was negatively correlated to quinate in leaves, and positively correlated to Glc-6-P, Fru-6-P and Fru in roots (Supplementary Table S2).

In the global correlation matrix, physiological trait-correlated metabolite Glc-6-P exhibited the most differentiated correlation profile, with no correlation with amino acids and, in contrast, with numerous correlations with carbohydrates (Fru-6-P, Tre, Suc, Fru) and stress-related metabolites (lactate, arabitol, sorbitol, ornithine, pipecolate) (Figs 7, 8, Supplementary Table S3). Nevertheless, considering modality-specific correlation matrices analyzing separately transfer and direct exposure-related data, Glc-6-P was negatively correlated to key metabolites previously identified by metabolite-physiological trait correlations (amino acids, TCA, stress metabolites, arabinose, quinate; Supplementary Table S4). This was also the case for Fru-6-P, which exhibited, for both transfer and direct exposure modalities, negative correlations to physiological parameter-correlated metabolites (Supplementary Table S4). Additionally, Fru was positively correlated to the same correlated metabolites, except Asn, in the global correlation matrix (Supplementary Table S3), thus highlighting the importance of soluble and phosphorylated sugars in metabolic responses to chemical stress.

The disaccharide Tre, whose levels generally increased in response to all types of chemical stress (except in the presence of tebuconazole), was characterized, like ribose, by a majority of negative correlations (25 against 5 positive correlations) (Figs 7, 8). Variations in Tre levels were closely linked with variations of almost all of previously-cited metabolites (Leu, Glc, Ser, succinate, Glc-6-P, Ala), thus suggesting a central role of Tre, as represented in Figure 8, in spite of low concentration and weak variations (Supplementary Figure S2). Tre was negatively linked to succinate, with depletions or increases of this highly variable TCA being associated, respectively, with increases or depletions of Tre in most cases (Figs 4, 7). Tre was negatively correlated to Glc, which could reflect direct transformation of Tre into Glc by trehalase. In contrast, no correlation was found between Tre and Suc, in contrast with studies showing parallel variations of Suc and Tre [or trehalose-6-phosphate (Tre-6-P)] (Lunn et al., 2014). One of the positive correlations exhibited by Tre was with its precursor Glc-6-P,

which can generate Tre-6-P and then Tre through combined activities of Trehalose-phosphate-synthase (TPS) and Trehalose phosphate phosphatase (TPP) (Figs 7, 8). However, comparison of relative levels of Tre and other correlated metabolites, such as Glc and Glc-6-P, did not show causal and strict relationships, thus suggesting that these convergent correlations could be attributed to more central regulatory roles for Tre, or Tre-6-P.

Considering correlation networks between soluble sugars (Fig. 8), the highest correlation was found for Glc-6-P and Fru-6-P, which exhibited similar increases in response to all of the chemical stressors, except glyphosate. Suc and Glc were positively correlated, their levels being increased by AMPA, and decreased by glyphosate, tebuconazole, or copper. The patterns of Glc and Fru, which are directly dependent on Suc metabolism, were similar for most chemical stress conditions. Nevertheless, correlation between Suc and Fru was not significant, thus suggesting that Glc and Fru levels could be regulated through stress mechanisms involving Glc-6-P and Tre pathways. A major feature of chemical stress response in *Lolium perenne* was therefore the modification of carbohydrate metabolism, leading to decrease of Suc, Glc (which are among the 13 highly variable metabolites with $Log_2(ratio)>1$ or <-1; Supplementary Figure S2, Fig. 5) or Fru levels, globally correlated with accumulation or maintenance of Tre, Fru-6-P and Glc-6-P.

Carbohydrate metabolism was linked to amino acid metabolism, with Tre being negatively correlated to Leu and Ser (Fig. 7). Leu decrease in leaves was associated to Tre accumulation in the presence of AMPA (Fig. 5). Leu belongs to branched-chain amino acids (BCAA; Ile, Leu, Val), which were grouped in cluster B, and were strongly interconnected. Simultaneous increase of Leu, Ile and Val levels in response to tebuconazole (Fig. 4), or their concomitant decrease in leaves under direct exposure in response to copper (Fig. 4), indicated coordinated changes of BCAA catabolism. Cluster B metabolites showed the greatest number of correlations with other metabolites. Leu was positively correlated to chlorophyll levels (Fig. 6) and to 27 metabolites, among which Ser and shikimate pathway derivative quinate.

Ser (cluster E) was among the most highly variable metabolites [$Log_2(ratio)>1$ or <-1; Supplementary Figure S2, Fig. 5] and was highly accumulated in response to fluoranthene and tebuconazole. Ser exhibited 33 significant correlations, among which there were only two negative cases, with Tre and ribose (Fig. 7), and was strongly positively correlated to Gly and Glu, which are close photorespiratory intermediates. Indeed, levels of these amino acids increased in response to most of the chemical stressors under at least one condition, except for glyphosate treatment and copper treatment where they decreased jointly (Fig. 5, Supplementary Figure S2). Ser was positively correlated to Asn and Ala, which constitute

amino group donors for synthesis of the photorespiratory intermediate Gly (Fig. 7). These correlations may confirm involvement of the photorespiratory pathway in chemical stress responses, and highlighted the importance of Ser. Photorespiration and N status, which were closely connected and regulated, thus seemed to play important roles in responses to chemical stress in Lolium.

DISCUSSION

Chemical stressors at subtoxic levels have major impacts on growth and metabolic composition

Subtoxic levels of chemical stressors induced significant physiological effects in *Lolium perenne*. The extent of these effects depended on type of pollutant, on modality of exposure, and on physiological trait. Parallel investigation of physiological modifications in roots and leaves for different chemicals highlighted primary impacts of chemical stressors on roots, the first organ exposed to stress, across various stressors and across various modes of action. Leaf-related parameters (leaf length, pigment contents), exhibited intermediary sensitivity to chemicals. In contrast, PSII efficiency (*Fv/Fm*) remained unaffected by the different treatments under conditions of transfer or direct exposures (Fig. 1D, H). Although a species-specific effect of *Lolium perenne* could not be excluded, this result suggests low sensitivity of PSII efficiency to low or sublethal levels of chemical stressors, contrasting with its wide use as chemical stress marker under high exposure level (Li et al., 2013; Mateos-Naranjo and Perez-Martin, 2013; Kreslavski et al., 2014). Low-intensity chemical stress therefore seems to act primarily on growth and development rather than on photosynthesis, thus suggesting that developmental processes may be important targets of subtoxic chemical stress.

Although transfer and direct exposures led to similar trends across treatments, in terms of physiological responses, direct exposure induced more pronounced effects than transfer exposure. These results could be related to intensity of chemical stress, and to levels of chemical stress sensitivity. Exposure modalities reflected different durations of exposure, with a nearly three times longer exposure for direct exposure. Exposure modalities differed in the developmental stage at which Lolium was submitted to chemicals, since direct exposure was applied to seeds, whereas transfer experiments affected 7-d-old plantlets.

Subtoxic levels of chemical stressors induced metabolic effects that did not overrun general metabolic signatures of plant organs and of exposure modalities (Supplementary Figure S1). Nevertheless, metabolic analysis of roots, which were the primary site of exposure, under direct exposure (Fig. 3C), which gave the most intense physiological effects (Fig. 1), revealed different types of chemical stress responses: i) a low-intensity response highlighted by AMPA, ii) a glyphosate response (G, GT) characterized by quinate accumulation, iii) a heavy-metal response characterized by citrate and succinate depletion, and iv) a cyclic-compound response (F, T), characterized by putrescine accumulation. These metabolic changes, not deeply altering the global plant metabolome, and occurring with maintenance of plant growth

(Fig. 2), were likely to reflect chemical stress adjustment rather than deregulation of homeostasis, leading, under long-term exposure, to avoidance of root growth inhibition for most of chemical stressors (glyphosate, tebuconazole, copper) (Fig. 2).

The effects of chemical stressors, such as those induced by AMPA, the degradation product of glyphosate, led to important changes of metabolic composition, especially affecting amino acid and sugar compositions, which are major components of ryegrass nutritional quality for herbivores (Barbehenn et al., 2004). It was noteworthy that such changes of metabolic composition could occur in the absence of major physiological impact, as was the case for transfer exposure and for some of the direct exposure treatments (Figs 1, 3), thus emphasising that assessment of chemical stress impact in the environment should integrate a wider range of parameters than PSII efficiency, chlorophylls or plant growth. Perennial ryegrass is a major component of grazed pastures and of grasslands, which cover a large fraction of Earth's land surface (Barbehenn et al., 2004). The chemical stressors that were shown in the present study to affect ryegrass, in terms of growth/biomass and of metabolite contents (i.e. soluble sugars, amino acids), are part of diffuse pollution problems associated with agriculture (Dévier et al., 2011). Discrete adjustments of grassland species to diffuse soil pollution may have important consequences on grassland functions, such as herbivore nutrition (Barbehenn et al., 2004), carbon sequestration and global change mitigation (Laliberté and Tylianakis, 2012). In this global context, understanding the mechanisms of ryegrass-xenobiotic interactions is of primary importance.

Comparative analysis reveals novel mechanisms of action of chemical stressors

Metabolomics has been used in pesticide and bioregulator research to study modes of action of chemicals and associated metabolic responses (Grossmann et al., 2012). Most studies have been carried out on one chemical or a few close chemicals affecting known cellular targets. The present work showed that parallel metabolomic investigation of different chemical stressors was useful to discover common and specific response patterns, including novel effects that could not be inferred from commonly-known modes of action. General chemical stress responses consisted in a systematic or frequent increase of key amino acids, among which N-rich amino acid Asn, branched-chain amino acids and Lys, and in a systematic decrease of glycerate and Ala (Figs 4, 5). Under chemical stress, *Lolium perenne* underwent metabolism reorganization rather than stress response induction, commonly characterized by stress metabolite accumulation (Fig. 6). None of the key metabolites involved in general chemical stress responses was significantly correlated to root or leaf physiological parameters

(Supplementary Table S2), thus suggesting that physiological responses may be more related to specific actions of each chemical stressor rather than to a general metabolic response.

Besides common responses, chemical stressors induced specific metabolite variations (Table 1), thus highlighting potential novel modes of action. Glyphosate, inhibitor of the shikimate pathway (Gomes et al., 2014), generated large accumulation of quinate in roots, contrasting with its absence of effects on aromatic amino acid levels (Phe, Tyr). Maintenance of these EPSPS inhibition markers could be ascribed to low level of glyphosate exposure (Serra et al., 2013). However, quinate accumulation in glyphosate-treated pea seedlings has been reported to result from glyphosate-induced modification of carbon flux in the direction of quinate synthesis (Orcaray et al., 2010). Glyphosate toxicity could originate from high quinate level in root, associated with shikimate pathway deregulation, leading to shoot and root growth inhibition (Orcaray et al., 2010; Zulet et al., 2013). This characteristic quinate accumulation was maintained under glyphosate-tebuconazole mixture, which resulted in root growth inhibition. Glyphosate also affects cell division in sea urchin by impeding activation of cell cycle regulator CDK1/cyclin B (Marc et al., 2002). Since CDKs and cell cycle checkpoints are universal in eukaryotes, root growth inhibition of *Lolium perenne* under glyphosate treatment may reflect action of glyphosate on root meristem activity and cell division. AMPA was also found to inhibit root growth (Fig. 1). However, analysis of related metabolic profiles indicated different modes of action in comparison to its parent compound glyphosate, since AMPA led to large quinate depletion in leaves (Fig. 5, Supplementary Figure S2). Such quinate variations could be due to shikimate pathway deregulation, or redistribution of carbon by this highly translocable carbon form (Orcaray et al., 2010). AMPA also led to arabinose decrease in roots (Fig. 5), clearly highlighting cell wall metabolism disturbance with potential significant impacts on root growth (Fig. 1). Given the structural analogy of AMPA with the amino acid Gly (Serra et al., 2013; Gomes et al., 2014), cell wall disturbance could originate from AMPA-induced imbalance in glycine-rich proteins (GRPs) in cell walls. GRPs are induced under stress and are hypothesized to interact with signalling pathways, thus suggesting a potential role as cell wall structure regulator (Caffall and Mohnen, 2009). Regarding Lolium metabolic profiles, AMPA altered Gly metabolism dynamics as previously reported (Serra et al., 2013). However, whereas it led to Gly depletion in *Arabidopsis thaliana* (Serra et al., 2013), it globally increased Gly levels in *Lolium perenne* (Fig. 5, Supplementary Figure S2).

Metabolic profiles induced by some chemical stresses confirmed previously reported modes of action. Copper treatment induced, under direct exposure, TCA depletion in roots, which

could originate from increasing energy demand for ATP-synthase and ATPase-dependent copper exclusion (Li et al., 2013; Lin et al., 2013), as well as from release of citrate- and succinate-containing root exudates for metal complexation (Meier et al., 2012). Tebuconazole, which decreases gibberellin levels by interacting with cytochrome P450 in the phytosterol biosynthesis pathway (Child et al., 1993; Lamb et al., 2001), also affected TCA levels (Table 1), as described by Ribeiro et al. (2012) in the case of paclobutrazol, a gibberellin biosynthesis inhibitor. TCA levels however varied differently, increasing in *Arabidopsis thaliana* leaves under paclobutrazol, being relatively unchanged in *Arabidopsis thaliana* seedlings under tebuconazole (Serra et al., 2013), and decreasing in *Lolium perenne* root under tebuconazole, thus showing species-specific triazole responses. Triazoles have been reported to induce abiotic stress tolerance (Horn et al., 2013), triazole-induced inhibition of gibberellin potentially affecting sugar-related signalling pathways and growth regulation (Child et al., 1993; Lamb et al., 2001). Tebuconazole was hypothesized to improve mRNA and protein stability and to induce compatible solute accumulation, leading to stress tolerance (Horn et al., 2013). Despite root growth inhibition, maintenance of high levels of pigment contents was found for T and GT treatments in comparison to G treatment (Fig. 1). Nevertheless, no clear accumulation of compatible solutes was observed (Fig. 5, Supplementary Figure S2), suggesting that interactions between chemicals may interfere with expected positive effects of tebuconazole. Indeed, effects of glyphosate-tebuconazole mixture likely resulted in a mix of deleterious effects of single chemicals, mainly characterized by inhibition of root and leaf growth associated with quinate and Asn accumulation, and TCA depletion (Figs 1, 4, 5, Supplementary Figure S2). Finally, increase of Ser levels by fluoranthene (Fig. 5) was in accordance with increase of glutathione levels reported by Kummerová et al. (2013) in pea and maize. In fact, fluoranthene, and more largely PAHs, generate, particularly in the meristem zones, reactive oxygen species, which must be detoxified (Zezulka et al., 2013; Kreslavski et al., 2014). Oxidation of membrane lipids by PAHs (Kreslavski et al., 2014) may lead to membrane disturbance that could explain the osmotic stress response observed in Lolium under fluoranthene treatment. This osmotic stress response was characterized by root growth enhancement (Fig. 1A, E) and leaf Pro accumulation (Fig. 5), as observed in Lolium seedlings under pyrene treatment (Chigbo and Batty, 2012), and by arabinose variations, which may reflect modifications of cell wall pectic fraction (Mustard and Renault, 2004). Association of fluoranthene and tebuconazole treatments into a cyclic-compound response under conditions of direct exposure (Fig. 3C, most intense physiological effects) may also be related to oxidative stress. Indeed, this

association was characterized by accumulation of the antioxidant compound putrescine (Scandalios, 2005), while fluoranthene generates reactive oxygen species (Kreslavski et al., 2014) and tebuconazole induces antioxidant systems (Zhang et al., 2010).

Reorientation of carbon and nitrogen metabolism is a major feature of chemical stress response

Our results showed that modifications in carbon and nitrogen metabolism were key factors in subtoxic chemical stress responses: (i) N-rich Asn was highly accumulated under most of the chemical stress conditions (Fig. 5, Supplementary Figure S2), (ii) Asn levels in roots were negatively correlated with leaf length (Fig. 6), (iii) Asn levels were positively correlated with levels of other amino acids (Fig. 7). In parallel, levels of either Glc, Fru or Suc decreased in response to each of the chemical stressors in at least one of the chemical stress conditions (Figs 4, 5; Supplementary Figure S2). Such differential dynamics of Glc, Fru and Suc could reflect modifications of carbon balance and carbon utilization, which were also suggested by effects of chemical stress on growth (Fig. 1) and on energy metabolism (Fig. 4). Further studies should determine whether changes of carbon balance entail higher synthesis of storage carbohydrates, as has been shown in *Lolium perenne* under other conditions of abiotic stress (Amiard et al., 2003).

Accumulation of Asn has generally been associated with different conditions of abiotic stress (mineral deficiencies, drought, salt, toxic metals) where the plant is unable to support normal protein synthesis (Lea et al., 2007; Maaroufi-Dguimi et al., 2011). Jia et al. (2001) have demonstrated that metsulfuron-methyl herbicide stress led to impairment of nitrogen metabolism and increase of Asn levels in soybean. Relationships between nitrogen metabolism and soluble carbohydrates have been shown in leaves of *Lolium perenne*, where nitrogen deficiency was associated with lower sucrose content (Lattanzi et al., 2012). *Oryza sativa* genotypes with contrasting tolerance to zinc deficiency and bicarbonate excess also exhibit decrease of Glc and Fru and increase of Asn, Asp, Gln, Val and Ile (Rose et al., 2012). The specific effects of chemical stressors therefore occur in association with perturbations of carbon-nitrogen homeostasis and trans-regulation of global amino acid metabolism, which may be part of global and common responses to environmental stresses.

Asn is important for nitrogen storage and transport from sources to sinks, especially under stress conditions of carbon limitation (Lam et al., 1998). Asparagine synthetase genes that are involved in Asn synthesis are regulated by levels of carbohydrates (Lam et al., 1998; Foito et al., 2013). Jia et al. (2001) suggested that Asn could be a signalling molecule involved in

sensing nitrogen status. Moreover, Asn has been characterized as an ammonia detoxification product (Lam et al., 1998; Lea et al., 2007). It would thus be important to determine whether, under conditions of subtoxic chemical stress, nitrogen mobilization is associated with ammonia toxicity and to what extent Asn accumulation plays a signalling role in orchestrating metabolic adjustments.

Asn, which is an amino group donor for synthesis of photorespiratory intermediate Gly, was positively correlated to Ser (Fig. 7). This was also the case for Ala, another amino group donor for photorespiration. Asn accumulation under chemical stress and such metabolic and functional correlations pointed out to involvement of photorespiratory pathway regulation in chemical stress responses in *Lolium perenne*, in line with previously-described effects of environmental stresses on other plant species (Ros et al., 2013), and highlighted the importance of Ser, which was recently described as a metabolic signal for transcriptional control of photorespiratory pathway genes in Arabidopsis (Timm et al., 2013). Photorespiration metabolism and nitrogen status, which are closely connected and co-regulated (Florian et al., 2013), are therefore likely to play important roles in responses to chemical stress in *Lolium perenne*, thus emphasising the need to improve current knowledge on photorespiratory processes in C3 grasses. Perturbations of nitrogen nutrition affect leaf growth of *Lolium perenne* (Kavanová et al., 2008). Because of the negative correlations between leaf growth and Asn and Ser levels in roots (Fig. 6), it would be important to investigate potential involvement of these two amino acids in root-shoot signalling, especially under chemical stress conditions primarily affecting root systems. It was noteworthy that a major common response to all of the chemical stressors was the depletion of two photorespiration-related compounds, Ala and glycerate (Florian et al., 2013). Given the importance of photorespiration increase in abiotic stress responses (Voss et al., 2013), this depletion may indicate potential perturbations of adaptive mechanisms in chemically-stressed ryegrass.

Coordination of chemical stress responses is associated with complex networks of correlations between amino acid and soluble sugar dynamics

The important metabolic changes described above were shown to be strongly interconnected (Figs 7, 8), thus indicating underlying mechanisms of regulation for coordination of amino acid, photorespiration and carbohydrate dynamics under conditions of subtoxic stress. As shown in Fig. 7, all of the metabolic response clusters were interconnected through significant correlations that converged towards cluster E, especially towards Ser, which showed an

extended network of positive correlations (Fig. 7), and towards Tre, which showed an extended network of negative correlations (Figs 7, 8). Ser was significantly correlated (Supplementary Table S3) with Glc (r = 0.76) and with Suc (r = 0.74). The dynamics of soluble sugars, Glc-6-P and Fru-6-P was structured as a Suc/Glc nexus in interaction with a Fru/Fru-6-P/Glc-6-P/Tre nexus, both nexus being centered on a negative Glc/Tre correlation (Fig. 8). All of these relationships suggested that stress-induced physiological and metabolic changes (Figs 6, 7) could be modulated by differential dynamics and interconversion of soluble sugars. The central position of these amino acid and soluble carbohydrate correlations, especially those involving Ser and Tre, revealed novel aspects of chemical stress responses that are seldom taken into account. Finally, the integration of Glc-6-P regulation in the network of soluble sugar dynamics could be related to the stability and buffering of Glc-6-P levels under subtoxic chemical stress (Fig. 5). The regulation of this stability may be an important determinant of the long-term adjustment of *Lolium perenne* to chemical stress (Fig. 2).

Such metabolic and physiological correlations can result from combinations of metabolic, regulatory and signalling relationships (Obata and Fernie, 2012). Glc-6-P is a major metabolic intermediate (Valluru and Van den Ende, 2011; Schluepmann et al., 2012) and an allosteric regulator of enzyme activities (Toroser et al., 2000). Glc-6-P can interact with signalling systems, as substrate for the synthesis of the signalling metabolite Tre-6-P (Lunn et al., 2014; Yadav et al., 2014) and as potential inhibitor of the energy sensor SNF1 (sucrose non-fermenting 1)-related kinase 1 (SnRK1) (Toroser et al., 2000; Valluru and Van den Ende, 2011; Nunes et al., 2013). Soluble carbohydrates involved in the central correlations described above (especially Glc, Suc, Tre) have been associated with signalling networks involving hexokinases (Granot et al., 2014), SnRK1 (Baena-González and Sheen, 2008; Dietrich et al., 2011; Lunn et al., 2014) or the target-of-rapamycin (TOR) kinase (Lastdrager et al., 2014; Xiong and Sheen, 2014). Ser is a metabolic signal for transcriptional control (Timm et al., 2013). All of these signalling regulations provide mechanisms of integration between growth, metabolism and stress responses in cross-talk with hormonal regulations (Valluru and Van den Ende, 2011; Xiong and Sheen, 2014). Their major effects consist in regulation of genes involved in catabolism (proteolysis, amino acid catabolism, sugar degradation, lipid mobilisation), especially of genes involved in Asn and BCAA metabolisms (Valluru and Van den Ende, 2011). As shown in the present work (Figs 4, 6, 7), changes of Asn and BCAA metabolisms were indeed important features of chemical stress responses in *Lolium perenne*. Further work is therefore needed to analyse relationships between regulation of amino acid

metabolism genes and SnRK1 functioning under conditions of subtoxic chemical stress.

Conclusions

Lolium perenne was therefore shown to undergo major metabolic changes under conditions of adjustment to chemical stresses and in the absence of major physiological and developmental alterations. These changes resulted in major reorientations of central carbon (sucrose, glucose, fructose) and nitrogen (asparagine, branched-chain amino acids, photorespiration) metabolisms. Some of these changes showed correlations with slight effects on physiological traits such as root length and leaf length. The extent of these metabolic responses did not however translate into long-term loss of fitness, thus reflecting adaptive flexibility of metabolism rather than deregulation of cellular and metabolic homeostasis. Moreover, this metabolic flexibility was shown to occur in response to diverse xenobiotic and heavy-metal stresses, indicating common underlying response mechanisms. These mechanisms were associated with complex correlation networks between amino acids and soluble sugars and with contrasted dynamic ranges of responses among closely-related metabolites. Carbohydrate metabolites such as sucrose showed important variations, in line with other situations of abiotic stress, whereas other key metabolites such as Glc-6-P followed a pattern of limited variations, which may thus be important links between metabolic flexibility and long-term tolerability to subtoxic chemical stresses. It was also noteworthy that parallel metabolomic analysis of diverse chemical stresses revealed common response patterns in a background of differing modes of action and stressor-specific mechanisms, thus suggesting that general lines of defence were induced under low-intensity chemical stress. However, given the wide range of ecosystemic functions associated with grasslands and pastures, higher-level impacts of metabolic changes in chemically-stressed *Lolium perenne* cannot be excluded.

SUPPLEMENTARY DATA

The following supplementary data are available in the online version of this article.

Figure S1. Principal component analysis (PCA) and hierarchical classification of global metabolic responses to chemical stressors.

Figure S2. Relative variations of levels of metabolites in *Lolium perenne* under chemical stress in comparison to control conditions (Log_2 ratio).

Method S1. Metabolite profiling method.

Table S1. Plant metabolites analysed by GC/MS method.

Table S2. Organ-specific physiological trait-metabolite and metabolite-metabolite correlation matrix.

Table S3. Global physiological trait-physiological trait, physiological trait-metabolite and metabolite-metabolite correlation matrix.

Table S4. Global and modality-specific Glc-6-P-metabolite and Fru-6-P-metabolite correlation matrix.

ACKNOWLEDGMENTS

This work was supported by interdisciplinary program ‘Ingénierie écologique’ [Centre National de la Recherche Scientifique (CNRS, France)] and by the Fondation pour la Recherche sur la Biodiversité (FRB, France). AAS is supported by a doctoral scholarship from the Brittany regional council (France).

We are grateful to Jean-Luc Foulon (Ecobio research unit) for help with plant culture systems and to Sandra Rigaud (Ecobio research unit) for administrative and accounting work.

REFERENCES

Amiard V, Morvan-Bertrand A, Billard JP, Huault C, Keller F, Prud'homme MP. 2003. Fructans, but not the sucrosyl-galactosides, raffinose and loliose, are affected by drought stress in perennial ryegrass. Plant Physiology **132**, 2218-2229.

Baena-González E, Sheen J. 2008. Convergent energy and stress signaling. Trends in Plant Science **13**, 474-482.

Barbehenn RV, Chen Z, Karowe DN, Spickards A. 2004. C3 grasses have higher nutritional quality than C4 grasses under ambient and elevated atmosphere CO_2. Global Change Biology **10,** 1565-1575.

Bidar G, Pruvot C, Garçon G, Verdin A, Shirali P, Douay F. 2009. Seasonal and annual variations of metal uptake, bioaccumulation, and toxicity in *Trifolium repens* and *Lolium perenne* growing in a heavy metal-contaminated field. Environmental Science and Pollution Research **16,** 42-53.

Caffall KH, Mohnen D. 2009. The structure, function, and biosynthesis of plant cell wall pectic polysaccharides. Carbohydrate Research **344,** 1879-1900.

Chigbo C, Batty L. 2012. Effect of combined pollution of chromium and benzo(a)pyrene on seed growth of *Lolium perenne*. Chemosphere **90,** 164-169.

Child RD, Evans DE, Allen J, Arnold GM. 1993. Growth responses in oilseed rape (*Brassica napus* L.) to combined applications of the triazole chemicals triapenthenol and tebuconazole and interactions with gibberellin. Plant Growth Regulation **13,** 203-212.

Couée I, Serra AA, Ramel F, Gouesbet G, Sulmon C. 2013. Physiology and toxicology of hormone-disrupting chemicals in higher plants. Plant Cell Reports **32,** 933-941.

D'Orazio V, Ghanem A, Senesi N. 2013. Phytoremediation of pyrene contaminated soils by different plant species. Clean-Soil, Air, Water **41,** 377-382.

Dear BS, Sandral GA, Wilson BCD. 2006. Tolerance of perennial pasture grass seedlings to pre- and post-emergent grass herbicides. Australian Journal of Experimental Agriculture **46,** 637-644.

Dévier MH, Mazellier P, Ait-Aissa S, Budzinski H. 2011. New challenges in environmental analytical chemistry: identification of toxic compounds in complex mixtures. Comptes Rendus Chimie **14,** 766-779.

Dietrich K, Weltmeier F, Ehlert A, Weiste C, Stahl M, Harter K, Dröge-Laser W. 2011. Heterodimers of the Arabidopsis transcription factors bZIP1 and bZIP53 reprogram amino acid metabolism during low energy stress. Plant Cell **23,** 381-395.

Dorato MA, Engelhardt JA. 2005. The no-observed-adverse-effect-level in drug safety evaluations: use, issues, and definition(s). Regulatory Toxicology and Pharmacology **42,** 265-274.

Florian A, Araújo WL, Fernie AR. 2013. New insights into photorespiration obtained from metabolomics. Plant Biology **15,** 656-666.

Foito A, Byrne S, Hackett CA, Hancock RD, Stewart D, Barth S. 2013. Short-term response in leaf metabolism of perennial ryegrass (*Lolium perenne*) to alterations in nitrogen supply. Metabolomics **9,** 145-156.

Gomes MP, Smedbol E, Chalifour A, Hénault-Ethier L, Labrecque M, Lepage L, Lucotte M, Juneau P. 2014. Alteration of plant physiology by glyphosate and its by-product aminomethylphosphonic acid: an overview. Journal of Experimental Botany doi:10.1093/jxb/eru269

Gonthier R, Francis D. 1989. Changes in the pattern of cell division in the shoot and root meristem of *Lolium perenne* during the transition from vegetative to floral growth. Journal of Experimental Botany **40,** 285-292.

Granot D, Kelly G, Stein O, David-Schwartz R. 2014. Substantial roles of hexokinase and fructokinase in the effects of sugars on plant physiology and development. Journal of Experimental Botany **3**, 809-819.

Grossmann K, Christiansen N, Looser R, Tresch S, Hutzler J, Pollmann S, Ehrhardt T. 2012. Physionomics and metabolomics - two key approaches in herbicidal mode of action discovery. Pest Management Science **68,** 494-504.

Helander M, Saloniemi I, Saikkonen K. 2012. Glyphosate in northern ecosystems. Trends in Plant Science **17,** 569-574.

Horn R, Chudobova I, Hänsel U, Herwartz D, Koskull-Döring PV, Schillberg S. 2013. Simultaneous treatment with tebuconazole and abscisic acid induces drought and salinity stress tolerance in *Arabidopsis thaliana* by maintaining key plastid protein levels. Journal of Proteome Research **12,** 1266-1281.

Hu C, Ou Y, Zhang D, Zhang H, Yan C, Zhao Y, Zheng Z. 2012. Phytoremediation of the polluted Waigang River and general survey on variation of phytoplankton population. Environmental Science and Pollution Research **19,** 4168-4175.

Hummel I, El-Amrani A, Gouesbet G, Hennion F, Couée I. 2004. Involvement of polyamines in the interacting effects of low temperature and mineral supply on *Pringlea antiscorbutica* (Kerguelen cabbage) seedlings. Journal of Experimental Botany **55,** 1125-1134.

Jia M, Keutgen N, Matsuhashi S, Mitzuniwa C, Ito T, Fujimura T, Hashimoto S. 2001. Ion chromatographic analysis of selected free amino acids and cations to investigate the change of nitrogen metabolism by herbicide stress in soybean (*Glycine max*). Journal of Agricultural and Food Chemistry **49,** 276-280.

Kavanová M, Lattanzi FA, Schnyder H. 2008. Nitrogen deficiency inhibits leaf blade growth in *Lolium perenne* by increasing cell cycle duration and decreasing mitotic and post-mitotic growth rates. Plant, Cell and Environment **31,** 727-737.

Kreslavski VD, Lankin AV, Vasilyeva GK, Luybimov VY, Semenova GN, Schmitt FJ, Friedrich T, Allakhverdiev SI. 2014. Effects of polyaromatic hydrocarbons on photosystem II activity in pea leaves. Plant Physiology and Biochemistry **81**:135-42.

Krutz LJ, Senseman SA, Zablotowicz RM, Matocha MA. 2005. Reducing herbicide runoff from agricultural fields with vegetative filter strips: A review. Weed Science **53,** 353-367.

Kummerová M, Zezulka Š, Babula P, Váňová L. 2013. Root response in *Pisum sativum* and *Zea mays* under fluoranthene stress: morphological and anatomical traits. Chemosphere **90,** 665-673.

Laliberté E, Tylianakis M. 2012. Cascading effects of long-term land-use changes on plant traits and ecosystem functioning. Ecology **93,** 145-155.

Lam HM, Hsieh MH, Coruzzi G. 1998. Reciprocal regulation of distinct asparagine synthetase genes by light and metabolites in *Arabidopsis thaliana*. Plant Journal **16,** 345-353.

Lamb DC, Cannieux M, Warrilow AG, Bak S, Kahn RA, Manning NJ, Kelly DE, Kelly SL. 2001. Plant sterol 14α-demethylase affinity for azole fungicides. Biochemical and Biophysical Research Communications **284,** 845-849.

Lastdrager J, Hanson J, Smeekens S. 2014. Sugar signals and the control of plant growth and development. Journal of Experimental Botany **65,** 799-807.

Lattanzi FA, Ostler U, Wild M, Morvan-Bertrand A, Decau ML, Lehmeier CA, Meuriot F, Prud'homme MP, Schäufele R, Schnyder H. 2012. Fluxes in central carbohydrate metabolism of source leaves in a fructan-storing C3 grass: rapid turnover and futile cycling of sucrose in continuous light under contrasted nitrogen nutrition status. Journal of Experimental Botany **63,** 2363-2375.

Lea PJ, Sodek L, Parry MAJ, Shewry PR, Halford NG. 2007. Asparagine in plants. Annals of Applied Biology **150,** 1-26.

Li G, Peng X, Xuan H, Wei L, Yang Y, Guo T, Kang G. 2013. Proteomic analysis of leaves and roots of common wheat (*Triticum aestivum* L.) under copper-stress conditions. Journal of Proteome Research **12,** 4846-4861.

Lin CY, Trinh NN, Fu SF, Hsiung YC, Chia LC, Lin CW, Huang HJ. 2013. Comparison of early transcriptome responses to copper and cadmium in rice roots. Plant Molecular Biology **81,** 507-522.

Lunn JE, Delorge I, Figueroa CM, Van Dijck P, Stitt M. 2014. Trehalose metabolism in plants. The Plant Journal **79**, 544-567.

Maaroufi-Dguimi H, Debouba M, Gaufichon L, Clément G, Gouia H, Hajjaji A, Suzuki A. 2011. An Arabidopsis mutant disrupted in *ASN2* encoding asparagine synthetase 2 exhibits low salt stress tolerance. Plant Physiology and Biochemistry **49,** 623-628.

Marc J, Mulner-Lorillon O, Boulben S, Hureau D, Durand G, Bellé R. 2002. Pesticide Roundup provokes cell division dysfunction at the level of CDK1/cyclin B activation. Chemical Research in Toxicology **15,** 326-31.

Mateos-Naranjo E, Perez-Martin A. 2013. Effects of sub-lethal glyphosate concentrations on growth and photosynthetic performance of non-target species *Bolboschoenus maritimus*. Chemosphere **93,** 2631-2638.

Meier S, Alvear M, Borie F, Aguilera P, Ginocchio R, Cornejo P. 2012. Influence of copper on root exudate patterns in some metallophytes and agricultural plants. Ecotoxicology and Environmental Safety **75,** 8-15.

Mustard J, Renault S. 2004. Effects of NaCl on water relations and cell wall elasticity and composition of red-osier dogwood (*Cornus stolonifera*) seedlings. Physiologia Plantarum **121,** 265-271.

Nunes C, Primavesi LF, Patel MK, Martinez-Barajas E, Powers SJ, Sagar R, Fevereiro PS, Davis BG, Paul MJ. 2013. Inhibition of SnRK1 by metabolites: tissue-dependent effects and cooperative inhibition by glucose 1-phosphate in combination with trehalose 6-phosphate. Plant Physiology and Biochemistry **63,** 89-98.

Obata T, Fernie AR. 2012. The use of metabolomics to dissect plant responses to abiotic stresses. Cellular and Molecular Life Sciences **69,** 3225-3243.

Orcaray L, Igal M, Marino D, Zabalza A, Royuela M. 2010. The possible role of quinate in the mode of action of glyphosate and acetolactate synthase inhibitors. Pest Management Science **66,** 262-269.

Ramel F, Sulmon C, Gouesbet G, Couée I. 2009. Natural variation reveals significant integration of carbohydrate nutritional status and acclimation to xenobiotic stress in *Arabidopsis thaliana* plantlets. Annals of Botany **104,** 1323-1337.

Ramel F, Sulmon C, Serra AA, Gouesbet G, Couée I. 2012. Xenobiotic sensing and signalling in higher plants. Journal of Experimental Botany **63,** 3999-4014.

Ribeiro DM, Araújo WL, Fernie AR, Schippers JH, Mueller-Roeber B. 2012. Translatome and metabolome effects triggered by gibberellins during rosette growth in Arabidopsis. Journal of Experimental Botany **63,** 2769-2786.

Ros R, Cascales-Miñana B, Segura J, Anoman AD, Toujani W, Flores-Tornero M, Rosa-Tellez S, Muñoz-Bertomeu J. 2013. Serine biosynthesis by photorespiratory and non-photorespiratory pathways: an interesting interplay with unknown regulatory networks. Plant Biology **15,** 707-712.

Rose MT, Rose TJ, Pariasca-Tanaka J, Yoshihashi T, Neuweger H, Goesmann A, Frei M, Wissuwa M. 2012. Root metabolic response of rice (*Oryza sativa* L.) genotypes with contrasting tolerance to zinc deficiency and bicarbonate excess. Planta **236,** 959-973.

Scandalios JG. 2005. Oxidative stress: molecular perception and transduction of signals triggering antioxidant gene defenses. Brazilian Journal of Medical and Biological Research **38,** 995-1014.

Schluepmann H, Berke L, Sanchez-Perez GF. 2012. Metabolism control over growth: a case for trehalose-6-phosphate in plants. Journal of Experimental Botany **4**, 1051-1068.

Serra AA, Nuttens A, Larvor V, Renault D, Couée I, Sulmon C, Gouesbet G. 2013. Low environmentally relevant levels of bioactive xenobiotics and associated degradation products cause cryptic perturbations of metabolism and molecular stress responses in *Arabidopsis thaliana*. Journal of Experimental Botany **64,** 2753-2766.

Servillo L, Giovane A, Balestrieri ML, Ferrari G, Cautela D, Castaldo D. 2012. Occurrence of pipecolic acid and pipecolic acid betaine (homostachydrine) in Citrus genus plants. Journal of Agricultural and Food Chemistry **60,** 315-321.

Timm S, Florian A, Wittmiß M, Jahnke K, Hagemann M, Fernie AR, Bauwe H. 2013. Serine acts as a metabolic signal for the transcriptional control of photorespiration-related genes in Arabidopsis. Plant Physiology **162,** 379-389.

Toroser D, Plaut Z, Huber SC. 2000. Regulation of plant SNF1-Related Protein Kinase by Glucose-6-Phosphate. Plant Physiology **123**, 403-411.

Valluru R, Van den Ende W. 2011. Myo-inositol and beyond - Emerging networks under stress. Plant Science **181,** 387-400.

Verbruggen N, Hermans C. 2008. Proline accumulation in plants: a review. Amino Acids **35,** 753-759.

Voss I, Sunil B, Scheibe R, Raghavendra AS. 2013. Emerging concept for the role of photorespiration as an important part of abiotic stress response. Plant Biology **15,** 713-722.

Xiong Y, Sheen J. 2014. The role of TOR signaling networks in plant growth and metabolism. Plant Physiology **164,** 499-512.

Yadav UP, Ivakov A, Feil R, Duan GY, Walther D, Giavalisco P, Piques M, Carillo P, Hubberten HM, Stitt M, Lunn JE. 2014. The sucrose-trehalose 6-phosphate (Tre6P) nexus: specificity and mechanisms of sucrose signalling by Tre6P. Journal of Experimental Botany **4**, 1051-1068.

Zezulka S, Kummerová M, Babula P, Váňová L. 2013. *Lemna minor* exposed to fluoranthene: growth, biochemical, physiological and histochemical changes. Aquatic Toxicology **140-141,** 37-47.

Zhang YJ, Zhang XA, Chen CJ, Zhou MG, Wang HC. 2010. Effects of fungicides JS399-19, azoxystrobin, tebuconazloe, and carbendazim on the physiological and biochemical indices and grain yield of winter wheat. Pesticide Biochemistry and Physiology **98,** 151-157.

Zulet A, Zabalza A, Royuela M. 2013. Phytotoxic and metabolic effects of exogenous quinate on *Pisum sativum* L. Journal of Plant Growth Regulation **32,** 779-788.

Table 1. ***Major metabolic effects of subtoxic levels of chemical stressors on*** **Lolium perenne.**

Chemical stressors and stress conditions are described in Figure 1. Physiological effects are shown in Figure 1. Major metabolic changes were identified from response patterns shown in Fig. 5 and Supplementary Figure S2.

Stressor	Physiological effects	Major metabolic modifications	Organ	Potential impact
AMPA	Root growth inhibition	Quinate depletion Asn accumulation Arabinose depletion	Leaf Root	N metabolism disturbance Stress-induced proteolysis Cell wall metabolism disturbance
Glyphosate	Root growth inhibition	Quinate accumulation	Root	Quinate toxicity
Glyphosate + Tebuconazole	Leaf growth inhibition Root growth inhibition	Quinate accumulation Asn accumulation	Root	Quinate toxicity N metabolism disturbance Stress-induced proteolysis
Tebuconazole	Leaf growth inhibition Root growth inhibition	Asn accumulation Citrate depletion Asn accumulation	Leaf Root	N metabolism disturbance Stress-induced proteolysis TCA limitation N metabolism disturbance Stress-induced proteolysis
Fluoranthene	Leaf growth inhibition Root growth enhancement	Fru accumulation Glc accumulation Asn accumulation Ser accumulation Pro accumulation Fru accumulation Glc accumulation Ser accumulation Arabinose accumulation	Leaf Root	C metabolism modification N metabolism disturbance Stress-induced proteolysis Osmotic stress response C metabolism modification N metabolism disturbance Cell wall metabolism modification
Copper	Root growth inhibition	Citrate depletion Succinate depletion	Root	TCA limitation Exogenous metal complexation

FIGURE LEGENDS

Figure 1. Effects of subtoxic levels of chemical stressors on *Lolium perenne*. AMPA (A), glyphosate (G), tebuconazole (T), glyphosate plus tebuconazole (GT), fluoranthene (F) and copper (Cu) were tested. Values (mean ± SEM) of root length (A, E), leaf length (B, F), chlorophyll and carotenoid levels (C, G) and PSII efficiency (*Fv/Fm*) (D, H) are shown. In transfer experiments, seedlings were grown during 7 d under control conditions and then transferred to fresh medium in the presence of chemical stressors for 4 d (A, B, C, D). In direct exposure experiments, seedlings germinated and grew in the presence of chemical stressors for 11 d (E, F, G, H). Statistical analysis between means were carried out using the Mann-Whitney-Wilcoxon test. Statistical significance of differences ($P \leq 0.05$) between treatments is indicated by different letters above bars.

Figure 2. Long-term effects of subtoxic levels of chemical stressors on *Lolium perenne*. Chemical stressors are described in Fig. 1. Treatments consisted of direct exposures where seedlings germinated and grew in the presence of chemical stressors for 30 d. Values (mean ± SEM) of root length after 30 d of growth are shown. Statistical analyses were performed as described in Fig. 1.

Figure 3. Principal component analysis (PCA) and hierarchical classifications of metabolic responses of *Lolium perenne* to chemical stressors according to condition of exposure and to plant organ. Chemical stress treatments are described in Fig. 1. PCA was carried out on the correlation matrix of averages of metabolite levels measured for two conditions of stress exposure and in two different organs: root (A, TR: root after transfer exposure) and leaf (B, TL: leaves after transfer exposure) metabolite levels for transfer experiments; root (C, DR: root after direct exposure) and leaf (D, DL: leaves after direct exposure) metabolite levels for direct exposure experiments. Position of chemical treatments, distribution of metabolic parameters on the first plane (Dim1 and Dim2) and corresponding hierarchical classifications are shown. Treatment groups obtained by hierarchical classifications are circled.

Figure 4. Heatmap and average linkage hierarchical clustering of chemical stress-responsive metabolites. Heatmap and hierarchical tree result from relative levels of the 42 metabolites under study [$\log_2$(metabolite level under stress/metabolite level in control)]

according to roots (R) and leaves (L), to six chemical stress treatments (A: AMPA, G: glyphosate, GT: glyphosate plus tebuconazole, T: tebuconazole, F: fluoranthene, Cu: copper) and to two stress exposures [transfer experiment (T) and direct exposure (D)]. The first two letters correspond, respectively, to the type of exposure and the type of tissue; the letter after the underscore corresponds to stress treatment. Metabolites are separated in different clusters (named A to H) according to hierarchical classification.

Figure 5. Effects of subtoxic levels of chemical stressors on root and leaf metabolite concentrations of *Lolium perenne*. Effects of AMPA (A), glyphosate (G), tebuconazole (T), glyphosate plus tebuconazole (GT), fluoranthene (F) and copper (Cu) on *Lolium perenne* are shown for direct growth, which induced greater impacts on all traits (Fig. 1). Values (mean ± SEM) of root metabolite levels and leaf metabolite levels in nmol mg^{-1} of DW are shown respectively in grey bars and light bars. For each metabolite, the corresponding cluster (as defined in Fig. 4) is indicated into brackets.

Figure 6. Involvement of metabolic correlations in the effects of chemical stressors. Organ-specific physiological trait-metabolite correlations are shown. For each metabolite, the corresponding cluster (as defined in Fig. 4) is indicated into brackets. For metabolites of cluster B, graphs correspond to underlined metabolites. Inserted graphs represent relative variations of physiological traits or metabolites against control conditions [$\log_2$(ratio)]. Each inserted graph shows, from left to right, changes in trait responses and in metabolite levels under direct growth and transfer exposure for each treatment (A: AMPA, G: glyphosate, GT: glyphosate plus tebuconazole, T: tebuconazole, F: fluoranthene, Cu: copper). The Pearson correlation coefficient (r) for each pair of parameters is shown. Asterisks indicate significant correlations: *P≤0.05, **P≤0.001, ***P≤0.0001.

Figure 7. Correlations of chemical-stress-related metabolic networks with carbohydrate, tricarboxylate and photorespiratory metabolites. Red and green filled arrows represent, respectively, positive and negative Pearson correlations between directly-connected metabolites; red and green hashed arrows represent, respectively, positive and negative Pearson correlations between indirectly-connected metabolites. For each cluster, a typical metabolite is shown. For each metabolite, the corresponding cluster (as defined in Fig. 4) is indicated into brackets. Shaded metabolites are correlated to physiological parameters (Fig. 6). BCAA: Branched-chain amino acids; PP: photorespiratory pathway; TCA: tricarboxylic

acid. The Pearson correlation coefficient (r) for each pair of metabolites is shown. Asterisks indicate significant correlations: *P≤0.05, **P≤0.001, ***P≤0.0001.

Figure 8. Integration of soluble sugar dynamics and Glc-6-P regulation. Red and green filled arrows represent, respectively, positive and negative Pearson correlations between directly-connected metabolites in a pathway; red and green hashed arrows represent, respectively, positive and negative Pearson correlations between indirectly-connected metabolites. Colorless arrows represent metabolic pathways without significant Pearson correlation. For each metabolite, the corresponding cluster (as defined in Fig. 4) is indicated into brackets. Shaded metabolites are correlated to physiological parameters (Fig. 6). The Pearson correlation coefficient (r) for each pair of metabolites is shown. Asterisks indicate significant correlations: *P≤0.05, **P≤0.001, ***P≤0.0001.

Figure 1.

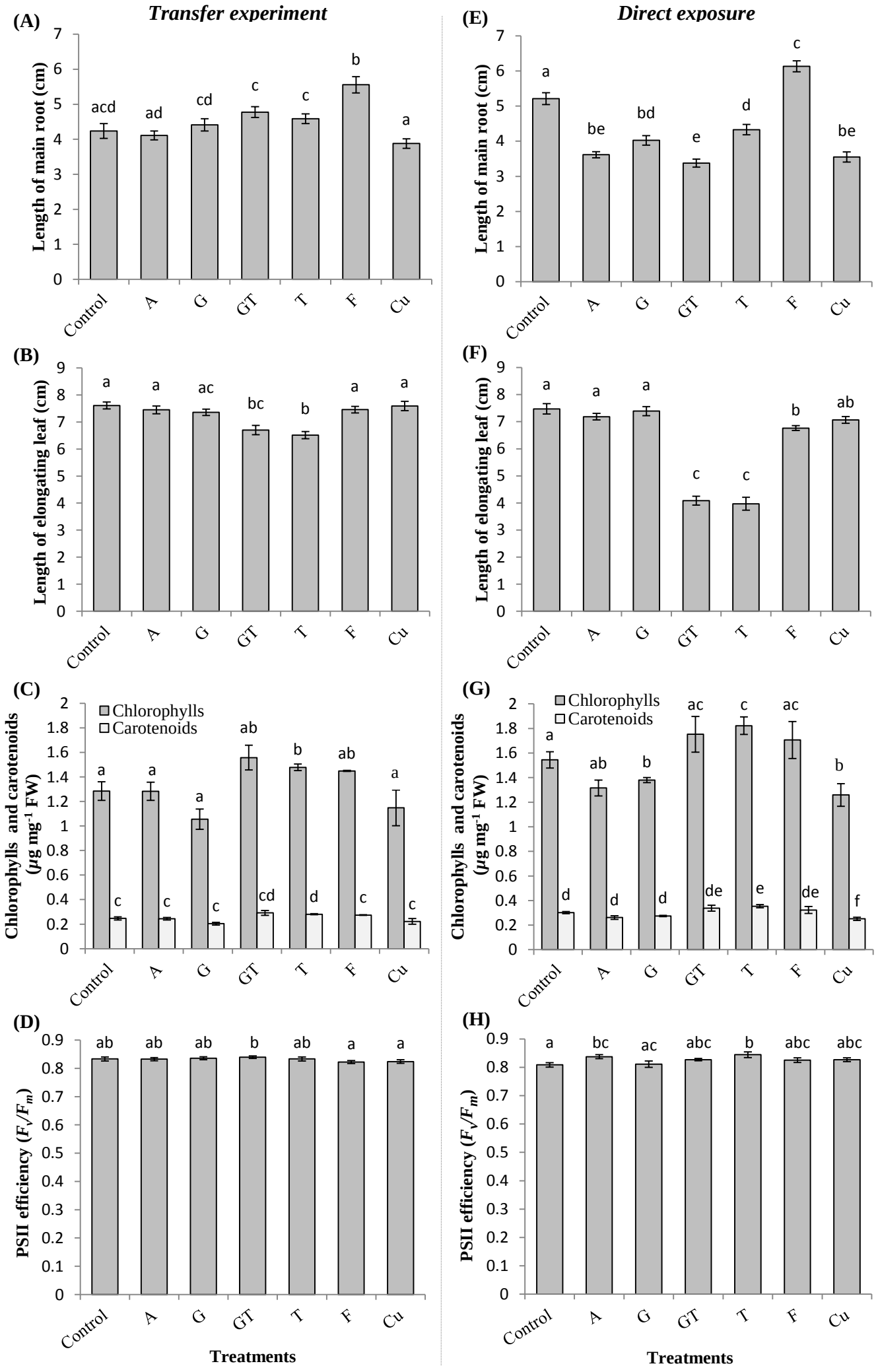
(A)
Transfer experiment
Length of main root (cm)
acd
ad
cd
c
c
b
a
(E)
Direct exposure
Length of main root (cm)
a
be
bd
e
d
c
be
(B)
Length of elongating leaf (cm)
a
a
ac
bc
b
a
a
(F)
Length of elongating leaf (cm)
a
a
a
c
c
b
ab
(C)
Chlorophylls and carotenoids (μg mg-1 FW)
Chlorophylls
Carotenoids
(G)
Chlorophylls and carotenoids (μg mg-1 FW)
Chlorophylls
Carotenoids
(D)
PSII efficiency (Fv/Fm)
ab
ab
ab
b
ab
a
a
(H)
PSII efficiency (Fv/Fm)
a
bc
ac
abc
b
abc
abc
Control
A
G
GT
T
F
Cu
Treatments

Figure 2.

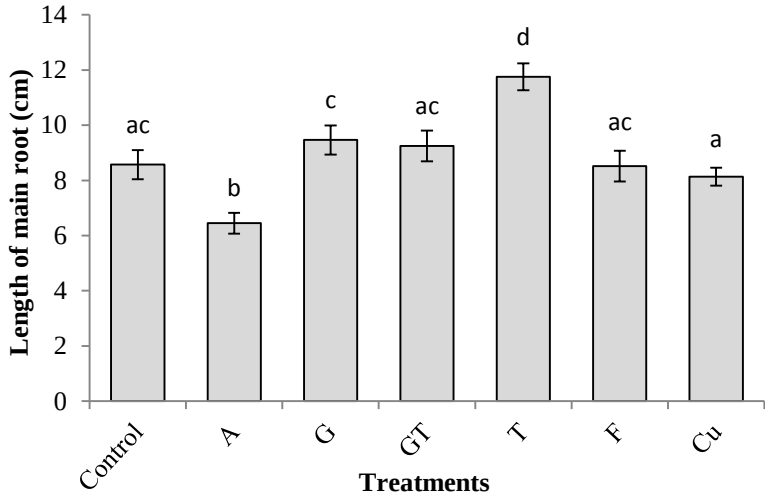
Length of main root (cm)
14
12
10
8
6
4
2
0
ac
b
c
ac
d
ac
a
Control
A
G
GT
T
F
Cu
Treatments

Figure 3.

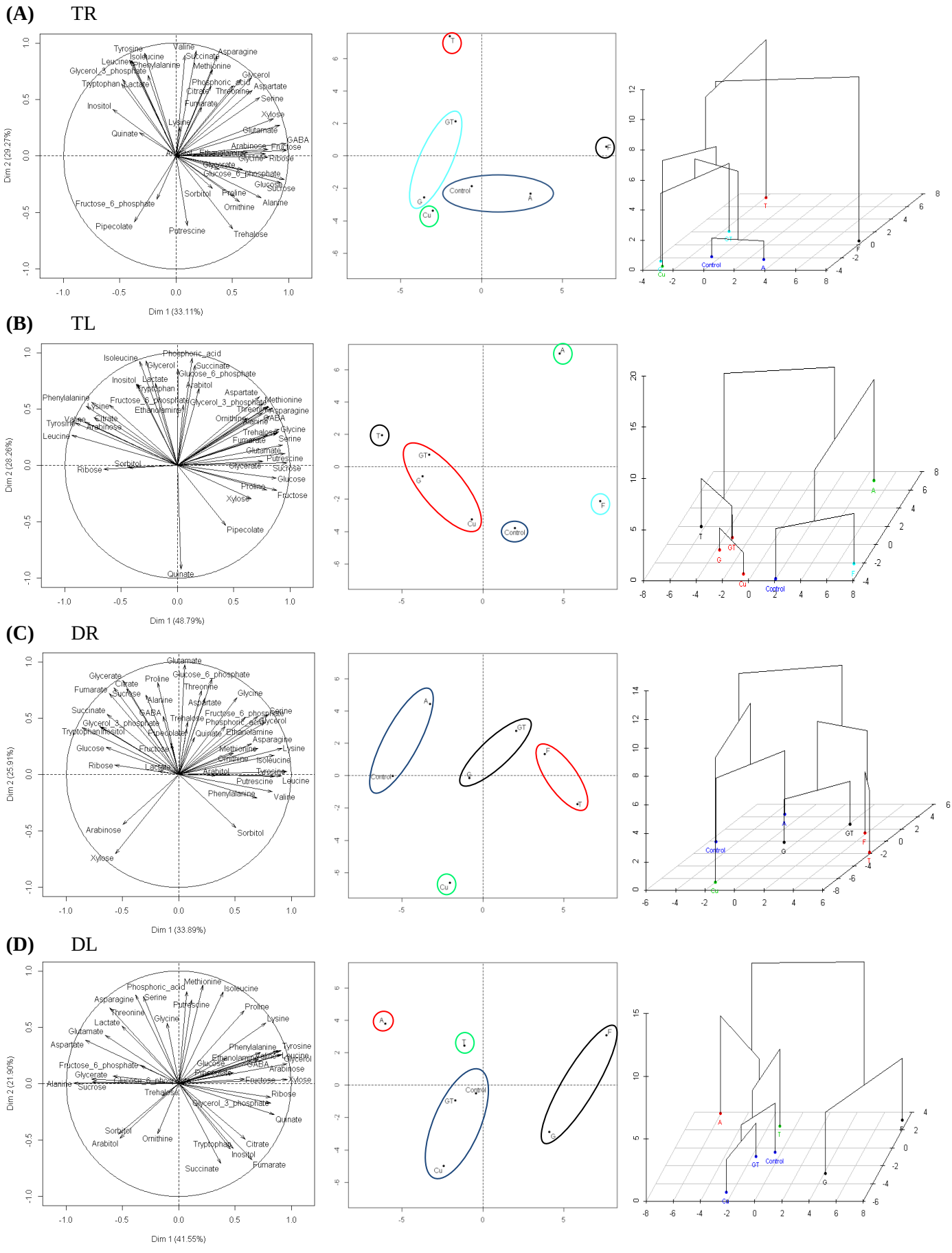
(A) TR
Dim 1 (33.11%)
Dim 2 (29.27%)
(B) TL
Dim 1 (48.79%)
Dim 2 (28.26%)
(C) DR
Dim 1 (33.89%)
Dim 2 (25.91%)
(D) DL
Dim 1 (41.55%)
Dim 2 (21.90%)

Figure 4.

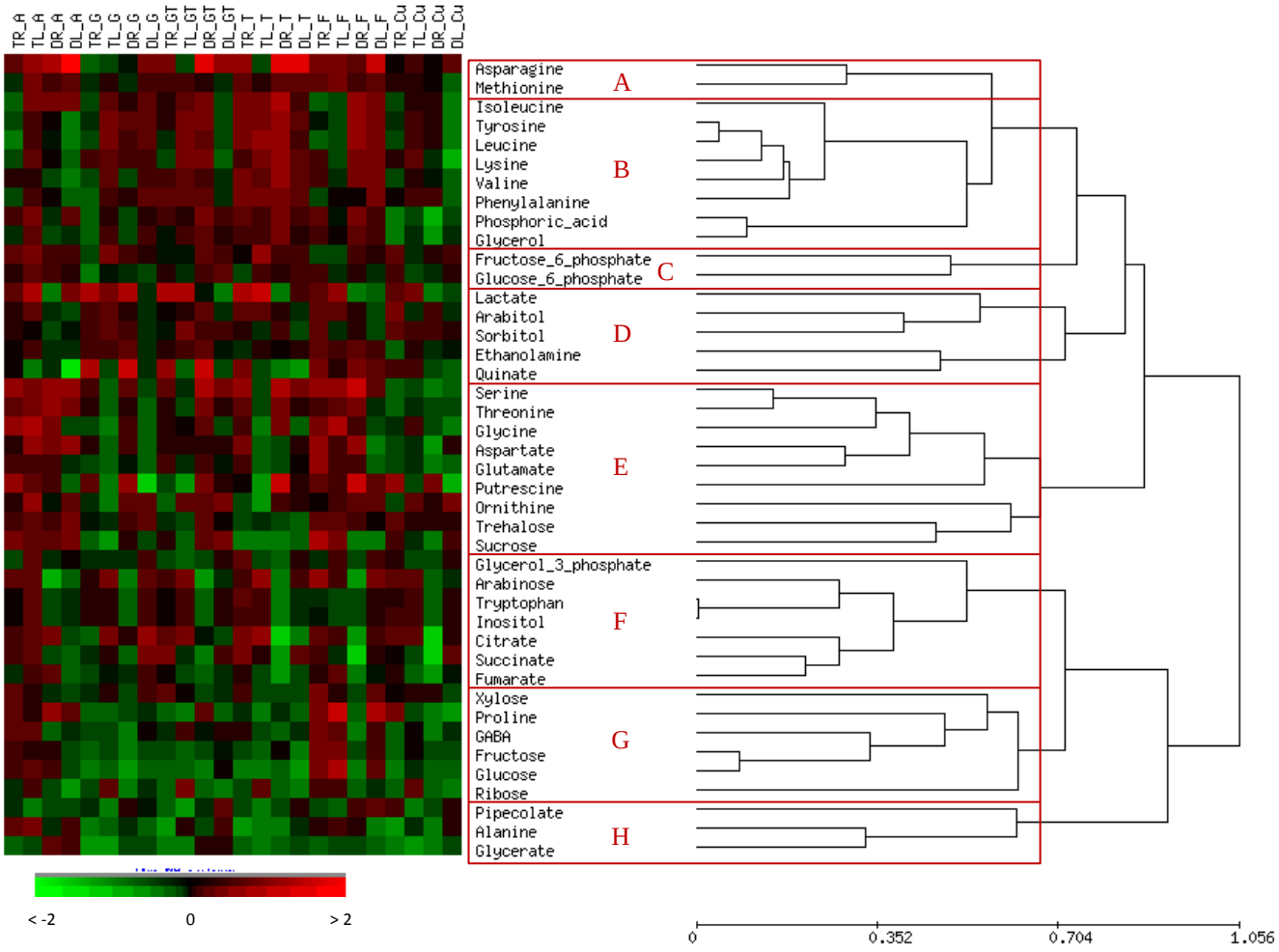
TR_A
TL_A
DR_A
DL_A
TR_G
TL_G
DR_G
DL_G
TR_GT
TL_GT
DR_GT
DL_GT
TR_T
TL_T
DR_T
DL_T
TR_F
TL_F
DR_F
DL_F
TR_Cu
TL_Cu
DR_Cu
DL_Cu
Asparagine
Methionine
A
Isoleucine
Tyrosine
Leucine
Lysine
Valine
Phenylalanine
Phosphoric_acid
Glycerol
B
Fructose_6_phosphate
Glucose_6_phosphate
C
Lactate
Arabitol
Sorbitol
Ethanolamine
Quinate
D
Serine
Threonine
Glycine
Aspartate
Glutamate
Putrescine
Ornithine
Trehalose
Sucrose
E
Glycerol_3_phosphate
Arabinose
Tryptophan
Inositol
Citrate
Succinate
Fumarate
F
Xylose
Proline
GABA
Fructose
Glucose
Ribose
G
Pipecolate
Alanine
Glycerate
H
< -2
0
> 2
0
0.352
0.704
1.056

Figure 5.

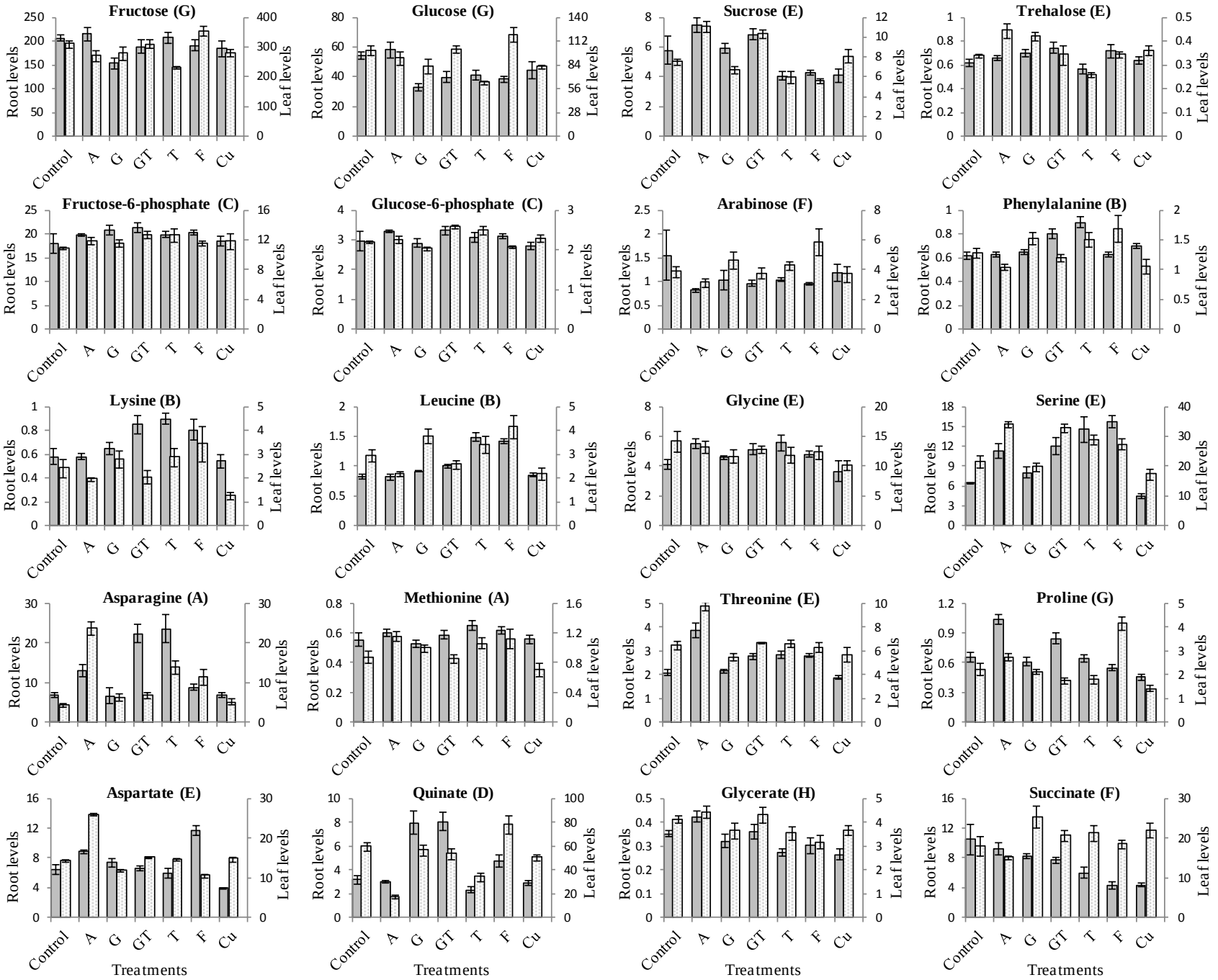
Fructose (G)
Glucose (G)
Sucrose (E)
Trehalose (E)
Fructose-6-phosphate (C)
Glucose-6-phosphate (C)
Arabinose (F)
Phenylalanine (B)
Lysine (B)
Leucine (B)
Glycine (E)
Serine (E)
Asparagine (A)
Methionine (A)
Threonine (E)
Proline (G)
Aspartate (E)
Quinate (D)
Glycerate (H)
Succinate (F)
Root levels
Leaf levels
Control
A
G
GT
T
F
Cu
Treatments

Figure 6.

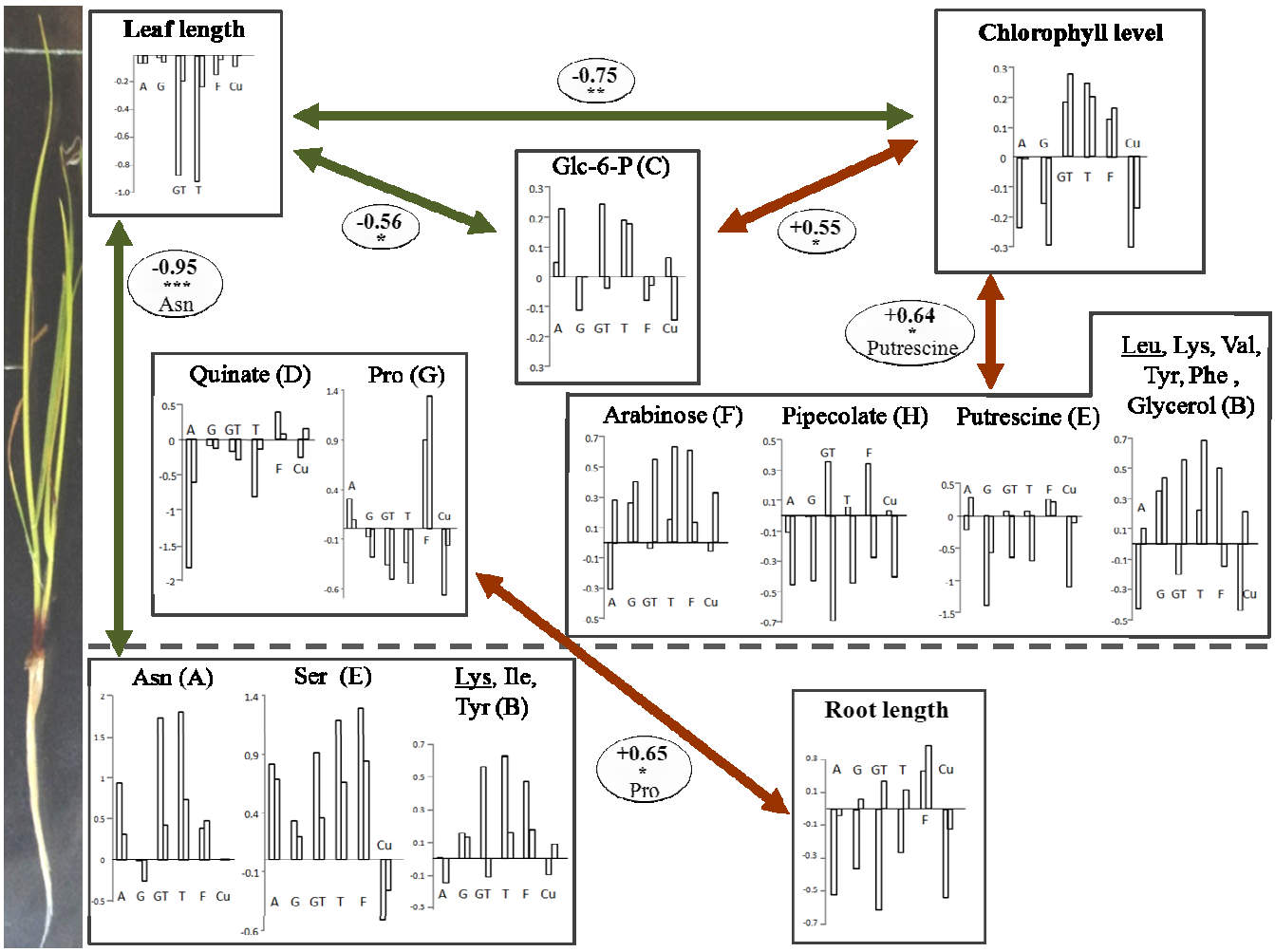
Leaf length
A G GT T F Cu
-0.75
**
Chlorophyll level
A G GT T F Cu
-0.56
*
Glc-6-P (C)
A G GT T F Cu
+0.55
*
-0.95
***
Asn
+0.64
*
Putrescine
Quinate (D)
A G GT T F Cu
Pro (G)
A G GT T F Cu
Leu, Lys, Val, Tyr, Phe , Glycerol (B)
Arabinose (F)
A G GT T F Cu
Pipecolate (H)
A G GT T F Cu
Putrescine (E)
A G GT T F Cu
Asn (A)
A G GT T F Cu
Ser (E)
A G GT T F Cu
Lys, Ile, Tyr (B)
A G GT T F Cu
+0.65
*
Pro
Root length
A G GT T F Cu

Figure 7.

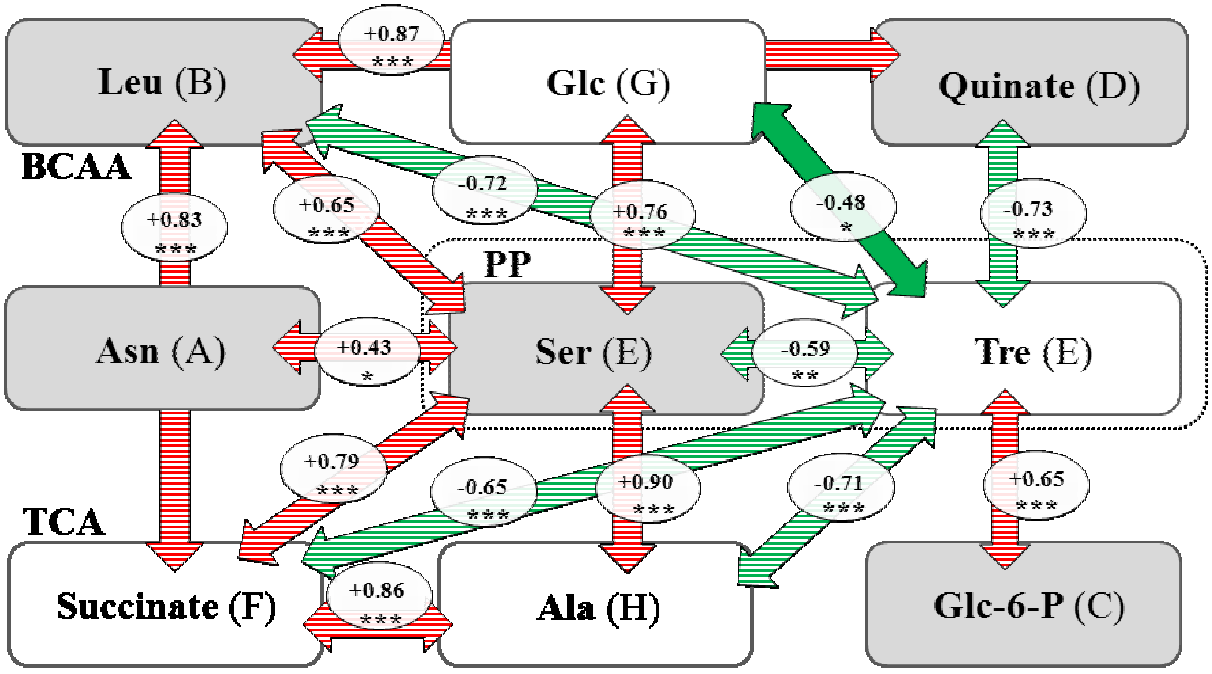
Leu (B)
Glc (G)
Quinate (D)
BCAA
Asn (A)
Ser (E)
Tre (E)
PP
TCA
Succinate (F)
Ala (H)
Glc-6-P (C)
+0.87 ***
+0.83 ***
+0.65 ***
-0.72 ***
+0.76 ***
-0.48 *
-0.73 ***
+0.43 *
-0.59 **
+0.79 ***
-0.65 ***
+0.90 ***
-0.71 ***
+0.65 ***
+0.86 ***

Figure 8.

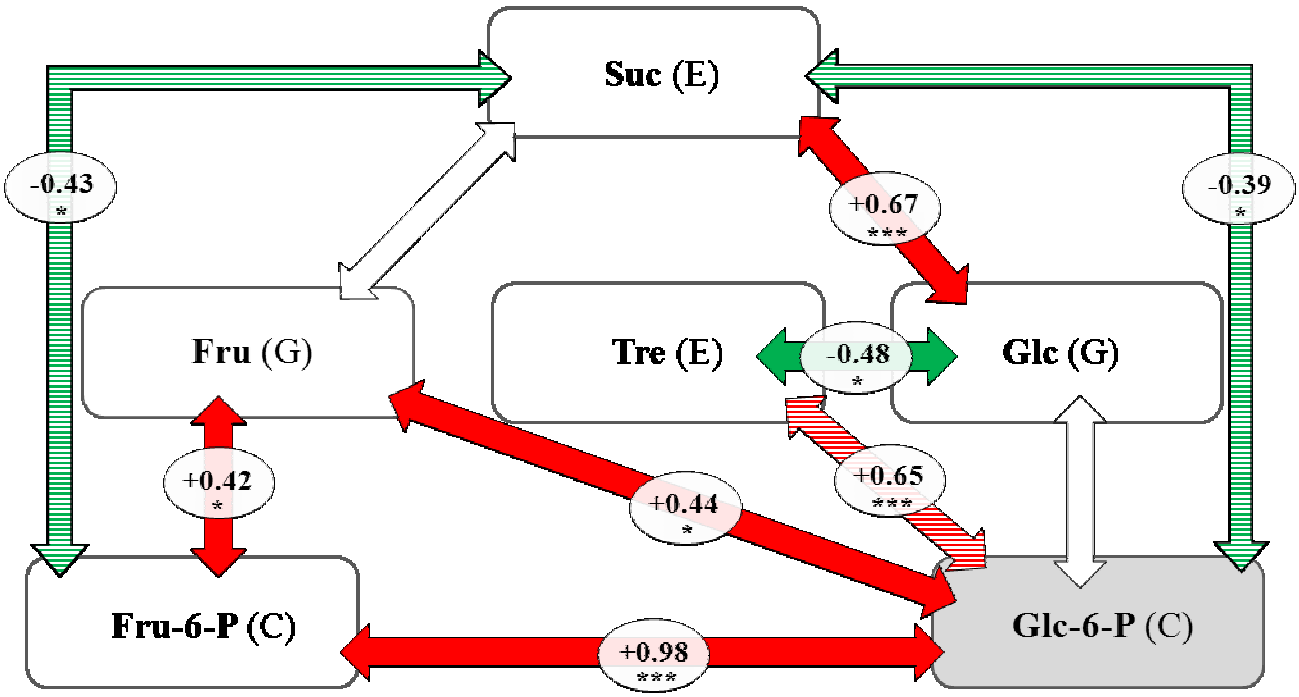
Suc (E)
-0.43
*
+0.67
***
-0.39
*
Fru (G)
Tre (E)
-0.48
*
Glc (G)
+0.42
*
+0.44
*
+0.65
***
Fru-6-P (C)
+0.98
***
Glc-6-P (C)

Manuscript Title: **Metabolic profiling of *Lolium perenne* shows functional integration of metabolic responses to diverse subtoxic conditions of chemical stress**

Author List: Anne-Antonella Serra, Ivan Couée, David Renault, Gwenola Gouesbet*, Cécile Sulmon*

Supplementary Method S1: Metabolite profiling method

Metabolite derivatization

The dried aliquots were re-suspended in 30 µL of 20 mg L-1 methoxyamine-pyridine solution, and placed under automatic orbital shaking at 40°C for 1 h. Thirty µL of N-methyl-N-trimethylsilyl trifluoroacetamide were added and derivatization was conducted at 40°C for 1 h under agitation. All the derivatization process was automatized using a CTC CombiPal autosampler (GERSTEL GmbH and Co.KG, Mülheim an der Ruhr, Germany), thus ensuring identical derivatization time and process for all samples.

Parameters of injection and of chromatography

The injector temperature was held at 250°C. The oven temperature ranged from 70 to 170°C at 5°C min-1, from 170 to 280°C at 7°C min-1, from 280 to 320°C at 15°C min-1. The oven then remained at 320°C for 4 min. A 30 m fused silica column (95% dimethyl siloxane, 5% phenyl polysilphenylene-siloxane, v/v) was used with helium as the carrier gas at a constant rate of 1 mL min-1. One microliter of each sample was injected using the split mode (25:1).

Supplementary Table S1: Plant metabolites analysed by GC/MS method

Amino acids	***Amines***
Alanine	Cadaverine
Asparagine	Dopamine
Aspartate	Ethanolamine
Citrulline	Putrescine
GABA	Spermidine
Glumatate	Spermine
Glycine	Triethanolamine
Isoleucine	Tyramine
Leucine	***Nucleobase***
Lysine	Cytosine
Methionine	***Organic acids***
Ornithine	Ascorbate
Phenylalanine	Citrate
Proline	Fumarate
Serine	Galactonolactone
Threonine	Glycerate
Tryptophane	Lactate
Tyrosine	Malate
Valine	Phosphoric acid
Oses	Pipecolate
Arabinose	Quinate
Fructose	Succinate
Fructose-6-phosphate	***Polyols***
Galactose	Arabitol
Galacturonic acid	Erythritol
Glucose	Galactitol
Glucose-6-phosphate	Glycerol
Maltose	Glycerol-phosphate
Mannose	Inositol
Ribose	Mannitol
Sucrose	Sorbitol
Trehalose	Xylitol
Xylose	

Supplementary Figure S1: Principal component analysis (PCA) and hierarchical classification of global metabolic responses to chemical stressors. Analysis was carried out on root (R) and leaf (L) metabolic responses of Lolium perenne to two types of chemical stress exposure [transfer experiment (T) and direct exposure (D)] to various chemical stressors as described in Fig. 1. PCA was carried out on the correlation matrix of averages of metabolite levels. The first two letters correspond, respectively, to the condition of stress exposure and the type of organ. The letter after the underscore corresponds to chemical treatment, as described in Fig. 1. The position of treatments (A), the corresponding hierarchical classification (B), and distribution of metabolic parameters on the first plane (Dim1 and Dim2; C) are shown. The four groups correspond to combinations of the two exposure modalities with the two organs: TR and TL for, respectively, root and leaves after transfer exposure, and DR and DL for, respectively, root and leaves after direct exposure.

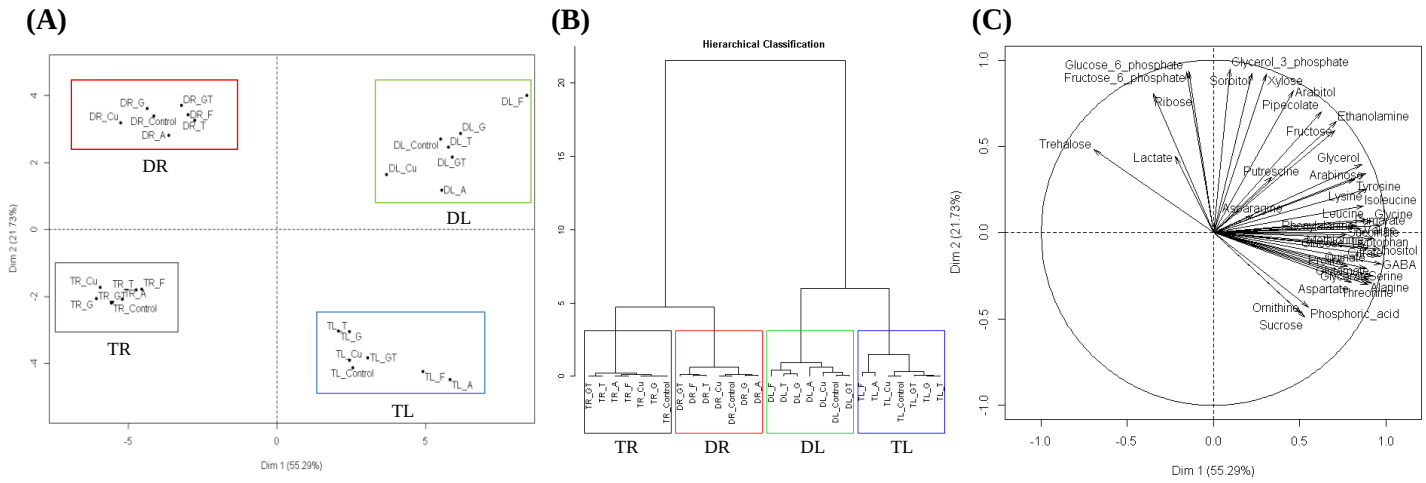

Supplementary Figure S2: Relative variations of the levels of metabolites in *Lolium perenne* under chemical stress in comparison to the control condition (Log2 ratio).

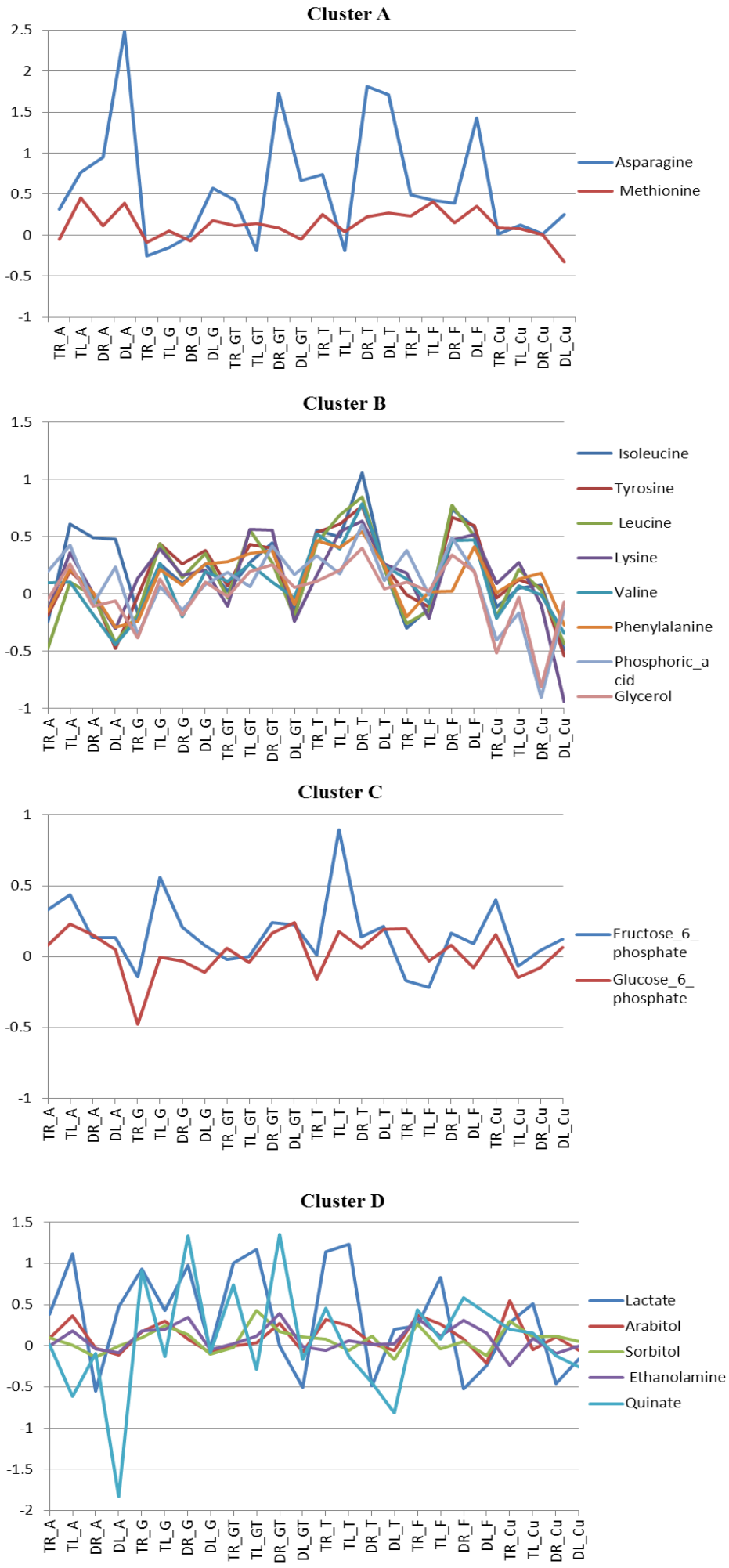

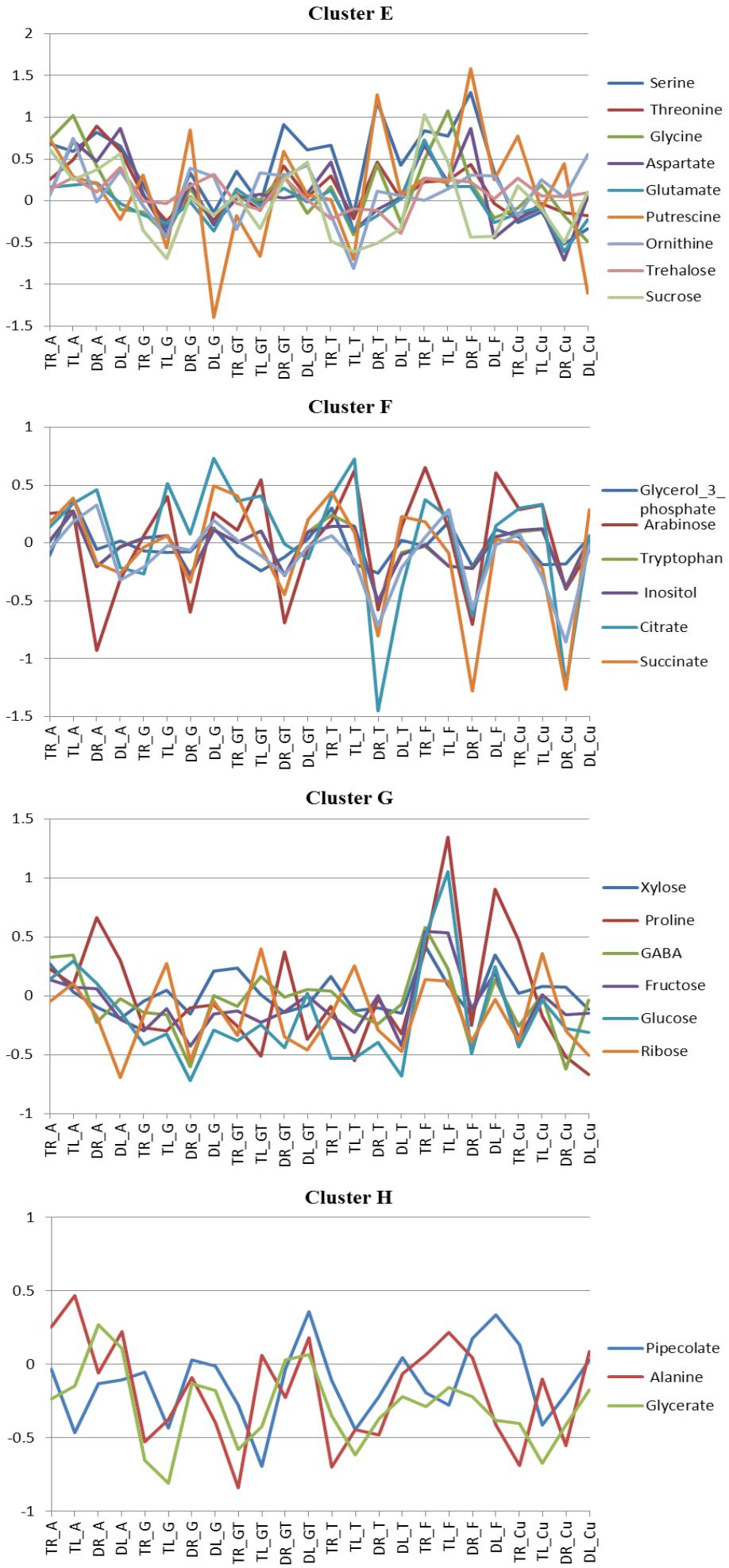
Cluster E
2
1.5
1
0.5
0
-0.5
-1
-1.5
TR_A
TL_A
DR_A
DL_A
TR_G
TL_G
DR_G
DL_G
TR_GT
TL_GT
DR_GT
DL_GT
TR_T
TL_T
DR_T
DL_T
TR_F
TL_F
DR_F
DL_F
TR_Cu
TL_Cu
DR_Cu
DL_Cu
Serine
Threonine
Glycine
Aspartate
Glutamate
Putrescine
Ornithine
Trehalose
Sucrose
Cluster F
1
0.5
0
-0.5
-1
-1.5
Glycerol_3_phosphate
Arabinose
Tryptophan
Inositol
Citrate
Succinate
Cluster G
1.5
1
0.5
0
-0.5
-1
Xylose
Proline
GABA
Fructose
Glucose
Ribose
Cluster H
1
0.5
0
-0.5
-1
Pipecolate
Alanine
Glycerate